Photometric Standardisation of Type Ia Supernovae: Evaluation and Potential Improvements Using Spectroscopic Data

Sam Blythe

PHYS450 Master's Project Report

April 27, 2025

Abstract

Type Ia Supernovae (SNe Ia) are powerful cosmological tools used to calibrate distance measurements. Due to an intrinsic brightness dispersion observed in their population, SNe Ia must undergo standardisation to be treated as standard candles. Current standardisation techniques make use of photometric data to employ empirical brightness corrections in order to reduce the average intrinsic dispersion in a sample. It is crucial to find ways to refine the standardisation process so that the accuracy of distance measurements is improved. This is essential for constraining cosmological parameters. This report evaluates the current widely used photometric correction parameters (α,β,γ) and explores spectroscopic data to find evidence for new corrections that could improve SNe Ia standardisation. A 4.79σ significant linear relationship was identified in the independent fit of photometrically standardised Hubble residuals against Si II λ6355 pseudo-equivalent width (pEW). This relationship could be evidence for a new standardisation correction. This was tested by including an additional correction term δW_λ^* in the typical $\alpha\beta\gamma$ standardisation regime, where δ is the fitted slope between residuals and pEW (W_λ^*). Fitting for α, β, γ, δ and intrinsic dispersion σ_{int} simultaneously yields a 5σ significant value of δ=0.0018$\pm$0.00036. The standard deviation of the SNe Ia sample used was reduced to 0.221 when applying the additional δ correction, down from 0.228 when using only α, β and γ. This could suggest that the new correction δ improves standardisation. However, the addition of the δ correction did not statistically significantly reduce the value of σ_{int} from the simultaneous fit for the SNe Ia sample. The value of σ_{int} for the $\alpha\beta\gamma\delta$ model may be overestimated due to simplification assumptions in the error calculation. These results may also be influenced by the presence of a selection bias in the SNe Ia sample used, which may need to be corrected for. Further research must be carried out, using a larger sample size, to accurately determine if this new correction can significantly reduce σ_{int}, and therefore improve SNe Ia standardisation. This report highlights that spectroscopic data has a great potential to enhance the SNe Ia standardisation process, which is crucial for advancing cosmology.

Statement of Contribution (For Markers' Use Only)

My supervisor provided the SNe Ia data (From Rigault et al., 2025 and Burgaz et al., 2025) in the form of csv files and gave guidance on ways this data could be used for my project. I developed Python programs that used pandas dataframes to read and manipulate this data. I used pandas dataframes to perform the data quality cuts suggested by Rigault et al. (2025) myself. I created 3 SNe Ia samples myself for this investigation using the full dataset (after quality cuts) provided in Rigault et al. (2025), a volume limited sample using a redshift cut suggested by Amenouche et al. (2025) and a subset of objects from the full sample for which spectroscopic data is available from Burgaz et al. (2025). All figures produced for this project were made using Python programs that I wrote myself using packages such as matplotlib, seaborn, and scipy (apart from Figs. 1 and 2 which are examples from the literature). The independent fitting process used to derive photometric corrections in Section 4 was done using Python codes developed by myself. The MCMC simultaneous fitting process introduced in Section 4.5 uses the skills developed from the Statistical Data Analysis in Physics module (hence, the explanation of this process is not too technical as it is assumed that the target audience for this report (my peers) will have also taken this module). However, all code for the simultaneous fits was developed and the data processed by myself. I made sure to include the most accurate uncertainty calculation found in the literature (Kessler and Scolnic, 2017). The bias investigation using K-S tests in Section 5 was also developed independently using skills from the data analysis module. I found evidence for the new spectroscopic correction suggested in Section 6 independently using my independent and simultaneous fitting Python programs. My suggestions for the impact this could have on improving standardisation and cosmology come from my detailed research on the literature and meetings with my supervisor.

Contents

1. Introduction

This report evaluates the use of spectroscopic techniques to standardise Type Ia Supernovae (SNe Ia). By analysing state-of-the-art data from the Zwicky Transient Facility (ZTF), this master's project investigates the use of additional spectroscopic corrections to supplement the empirical photometric corrections that are currently widely-used to standardise SNe Ia luminosities. The significant implications this has for cosmology will be discussed, along with suggestions for improvements and future areas of work.

Accurately measuring distances in the universe is an essential foundation of our current understanding of cosmology. This is because by using SNe Ia as a principal tool, the distances they derive can be used to determine many important cosmological parameters. For example, current methods to measure the accelerated expansion rate of the universe, the Hubble-Lemaître constant H_0, utilise SNe Ia derived distances (e.g., Freedman, 2021; Riess et al., 2022). Most famously, SNe Ia distances were used to infer the existence of dark energy in the 1990s (Riess et al., 1998; Perlmutter et al., 1999). Many other recent groundbreaking research studies also employ SNe Ia derived distances to measure cosmological parameters (e.g., Planck Collaboration, 2020; DESI Collaboration, 2025). Important examples of derived cosmological parameters include the mass density parameter Ω_m and the dark energy equation of state parameter ω which are discussed further in Section 2.3. These studies facilitate a deeper understanding of the size, age, structure, and composition of our universe. The more accurate measurements of distance are, the more constrained the measurements of cosmological parameters become (Guy et al., 2007) and, therefore, the better our understanding of the universe as a whole. This is the main motivation for this work and it places great importance on ensuring that distances in the universe are measured correctly. However, it raises the profound question: How do you ensure that distances in the universe are measured accurately?

On the cosmological scale, classic methods for measuring distances in astronomy, such as the parallax method, are no longer viable (the parallax angle becomes too small to use). Instead, utilisation of 'standard candles' is preferred. Standard candles are objects with a known standard brightness at a set distance which can be used to calibrate distance measurements. In reality, such objects do not exist in nature. Instead, standardisation methods must be applied to a group of similar objects in order to lower their dispersion to a reasonable level. The accuracy of the standard brightness depends on how effectively the standardisation process reduces the dispersion. If the standard brightness is accurately known, when one standard candle appears dimmer than another to a distant observer, it must be further away. This relationship is described by the equation,

$$M = m - 5\log_{10}(d) + 5 \tag{1}$$

where M is absolute (standard) brightness, m is the observed brightness and d is the distance measured in parsecs. Hence, it is incredibly important to refine the standardisation process in order to get an accurate measurement of the standard brightness to derive distances and important cosmological parameters. The next important question to ask therefore is: What objects have standardisable luminosities?

The breakthrough solution to this question is to use a specific event with a known standardisable brightness rather than a particular type of object. The event in question is a special type of supernova (the cataclysmic explosion caused when a star dies) known as a Type Ia supernova. Supernova events are naturally strong candidates for calibrating distance measurements as a result of the immense power of their explosion. They can briefly outshine even whole galaxies, meaning they can be detected at huge distances. Moreover, SNe Ia are known to explode

with roughly the same standard brightness (Branch and Tammann, 1992). The mechanisms behind this are still not fully understood (e.g., Wheeler and Harkness, 1990; Maoz et al., 2014), though the most popular and currently generally accepted theory is that SNe Ia are caused by the interaction between a carbon-oxygen white dwarf and a companion star in a binary system (e.g., Whelan and Iben Jr, 1973; Iben Jr and Tutukov, 1984; Nugent et al., 2011). It is thought that the white dwarf accretes matter from the companion star until it reaches a critical mass known as the Chandrasekhar Mass ($M_{ch} \approx 1.38\,\mathrm{M}_{\odot}$ (Chandrasekhar, 1931)). Once a white dwarf reaches this critical point, the high temperatures ignite nuclear reactions that lead to a runaway thermonuclear explosion (Mazzali et al., 2007; Liu et al., 2023). This is what we observe as a Type Ia supernova.

The fact that SNe Ia are caused by similar progenitor stars, occur at the same critical mass, and have almost consistent absolute brightness makes them perfect candidates to be standard candles. However, standardisation is still a necessary step because, despite their homogeneous nature, observed SNe Ia luminosities still exhibit a statistically significant intrinsic dispersion (e.g., Phillips, 1993; Hamuy et al., 1995). This natural dispersion has many different causes such as dust between the observer and the event absorbing light (e.g.,Brout and Riess, 2024) and differences in the compositions of the progenitor systems or explosion mechanisms (e.g., Hillebrandt and Niemeyer, 2000; Jha et al., 2019) which cause intrinsic luminosity variation. Factors such as these are ideally corrected for during the standardisation process. However, current methods employ empirical photometric corrections (e.g., Phillips, 1993; Tripp, 1998; Guy et al., 2007) that are not fully understood and standardise populations in general ways, sometimes without using direct measurements from the supernovae themselves. For example, the root cause of the 'host-step' correction (e.g., Kelly et al., 2010; Sullivan et al., 2010) is still widely up for debate (e.g., Wiseman et al., 2023; Chung et al., 2024), as outlined later on in this report (Sections 2 and 4.3). Another limitation of these corrections is the fact that the mechanisms responsible for the occurrence of SNe Ia are not yet fully understood (e.g., Maoz et al., 2014). If the standardisation process does not sufficiently reduce the dispersion of observed SNe Ia luminosities, then distance measurements become less accurate, which, as discussed earlier, has severe consequences for cosmology. For example, in the study by (Riess et al., 2022) it was shown that there is a 5σ difference between direct measurements of H_0 derived using standardised SNe Ia and theoretical expectations anchored from cosmic microwave background (CMB) data. Therefore, it is extremely important to find ways to improve the standardisation process so that these inconsistencies can be nullified.

One way in which standardisation could be improved is by using direct spectroscopic measurements from the supernovae themselves (e.g., Bailey et al., 2009) and investigating whether new and more effective corrections can be made using this data. As spectroscopic measurements come directly from the supernovae, they do not have the same pitfalls as the empirical photometric corrections. For example, spectroscopy explicitly tells us more about the composition of the star than photometry. Furthermore, it is not as negatively impacted by the presence of dust (see Section 2.1). This approach may bring us closer to correcting the data for phenomena that are more likely to be the root cause of dispersion, e.g. variation in the progenitor star composition. Other recent studies have also had success applying spectroscopic data to their standardisation methods in different ways (e.g.,Dixon et al., 2022; Martin et al., 2024). However, using spectroscopic data still has limitations. Supernova spectra take significantly longer to produce than light curves derived from photometry, which takes up valuable time on telescopes. Also, it is not always possible to produce a spectrum for objects that are very faint. This may introduce a bias towards brighter objects in the data capture process which could impact the validity of the results obtained from spectroscopic data.

The primary objective of this master's project was to investigate current SNe Ia standardisation methods and ascertain if they can be improved by using different cutting-edge spectroscopic techniques. If standardisation can be improved and the dispersion of SNe Ia luminosities lowered, then the measurement of the absolute brightness of SNe Ia is more accurate. This contributes towards the ultimate goal of improving distance measurements and therefore improving cosmology. The main aim of this report is to persuade the reader that spectroscopic techniques can be successfully employed to improve SNe Ia standardisation processes. Furthermore, it will be shown that, in spite of the fact that spectroscopic analysis is more expensive and time consuming than current photometric techniques, it is worth investing in such studies in the future to investigate this area more thoroughly and build upon the groundwork laid out in this report.

The main goal of this report will be achieved by first covering standardisation techniques in more detail in Section 2, to provide the reader with more in-depth context and necessary background theory. Then, Section 3 outlines the source of the SNe Ia data used throughout the project and will explain statistical analysis techniques used. Section 4 presents the results obtained when the current standardisation techniques are applied to the dataset to evaluate the best method to use. Section 5 analyses the validity of the data used due to the presence of selection bias. Section 6 introduces a new spectroscopic standardisation correction and its effectiveness will be compared with current methods. The discussion in Section 7 will consider the physical origins of spectroscopic corrections, their potential to improve standardisation and the wider impact this has on cosmology. Then, suggestions for future work will be proposed by improving and expanding on the work from this project. Finally, conclusions from this report will be given in Section 8.

2. Current SNe Ia Standardisation Techniques

This section provides more details on the prevailing photometric corrections that can be applied to a sample of SNe Ia in order to standardise their brightness. To begin with, it is first necessary to discuss what is meant by SNe Ia classification and to distinguish between spectroscopy and photometry (Section 2.1). The discovery and application of each photometric correction is then outlined in Section 2.2. Finally, Section 2.3 summarises the most up-to-date values of SNe Ia standardisation parameters found in the literature from recent investigations. This will be used to demonstrate the current best understanding of SNe Ia standardisation to compare with the results from this investigation. In summary, the aim of this section is to provide the reader with all necessary background information on SNe Ia standardisation before the methods and results from the master's project investigation are discussed.

2.1 SNe Ia Classification

Currently, supernovae are classified based on their spectral features, and standardised using photometric data. This report evaluates the use of spectroscopic data as an additional improvement to SNe Ia standardisation.

All objects in the universe that emit light that can be observed produce a unique spectrum of light that can be analysed. When a supernova event occurs, the immense energy from the explosion means that this spectrum of light can be detected from huge distances. The detected light is passed through a dispersive medium that breaks it up into its constituent wavelengths. A spectrum can be produced by plotting the intensity of light against wavelength. This allows analysis of light over a broad wavelength range, meaning that characteristic spectral features can be spotted easily. This provides a deep insight into the composition and mechanisms

behind the object producing the light, as certain absorption troughs or emission peaks in the spectrum correspond to specific chemical elements. Also, the ability to identify these spectral features is not too negatively impacted by interstellar dust. This is because dust relations involve adding lower-order polynomials to the function of the spectra and this does not change the relative shape of important spectral features (peaks, troughs, etc.) at local levels as these are represented using much higher order polynomials. This means spectral features can still be identified despite the presence of dust which makes spectroscopy incredibly useful. The main drawback of this method, however, is that because spectroscopy involves separating the light out into its constituent parts, it is 'spread thinly' over the detector. It therefore becomes difficult to detect multiple objects in one go. To get enough light to produce a spectrum, the detector must gather as much light as possible from one object at a time. This means that producing spectra takes up a lot of valuable time on telescopes.

Despite every spectrum being unique (due to slight inhomogeneities in an object's environment or composition), certain common features, shapes, or patterns can be identified in the spectra of similar objects. This forms the basis for supernova classification. SNe Ia are primarily classified by the absence of hydrogen lines in their spectra and a prominent silicon (Si II) absorption feature around 6100 Å (e.g., Harkness and Wheeler, 1990; Gal-Yam, 2016). This is due to the fact that a carbon-oxygen white dwarf, the likely progenitor for SNe Ia, contains no hydrogen, and silicon is a common by-product of the nuclear reactions that occur within them (Kato et al., 2018). Fig. 1 provides examples of typical supernova spectra for reference, with the Si II feature clearly noticeable on the SN Ia spectrum.

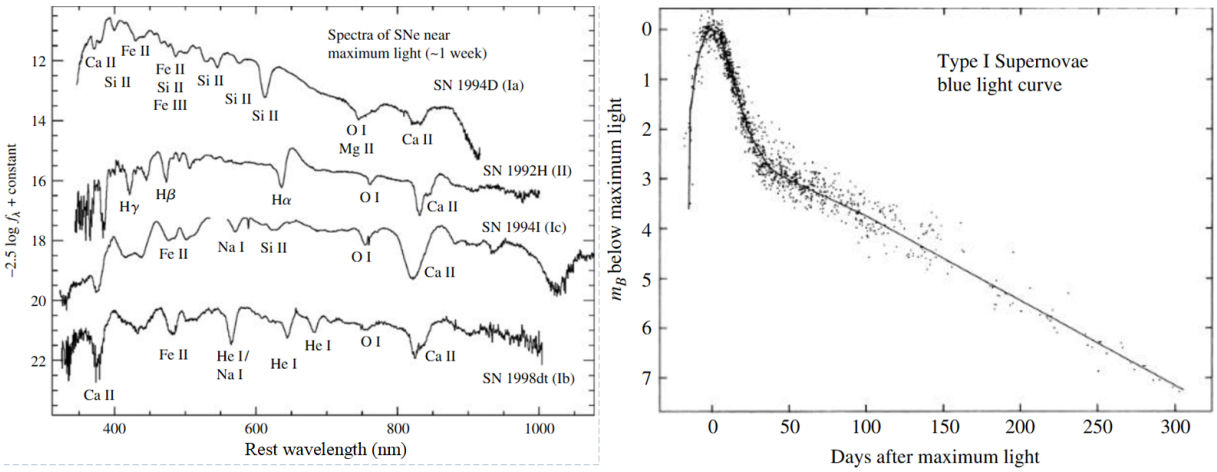

Figure 1: Example SNe spectra (LEFT) and light curves (RIGHT) from Carroll and Ostlie (2017) to demonstrate the differences in spectroscopic and photometric data. The spectrum of SN 1994D is observed to have a strong Si II absorption feature and no hydrogen lines and is therefore classified as typical Type Ia Supernova.

In contrast, photometry does not involve a detailed analysis of spectral features and instead focuses on the intensity of light. Images of the object are captured after the light is passed through specific colour filters and the flux (intensity) of light that is admitted through can be measured. The intensity of the filtered light recorded over time can then be plotted to produce a 'light curve'. Light curves show how the brightness of an object or event varies with time, and its shape can be used to understand more about the nature of the object producing the light. The main advantage of this method is that the image used can contain multiple sources of light, which results in much faster analysis. An example SN Ia light curve is shown in Fig. 1 with a peak luminosity corresponding to the time of peak emission (parametrised as t_0) from

the supernova remnants. All spectra used in this investigation are taken at t_0 which is known as 'nebula spectroscopy'. It is the emission from the chain of nuclear reactions of the heavier elements produced by the supernova that we observe - not the explosion itself. More specifically, it is high energy photons from the radioactive decay of elements like nickel or cobalt that are responsible for the peak in the light curve. The brightness drops off after this peak as these elements are used up, and the supernova remnants decay into elements that emit lower energy photons. Different SNe Ia events have similar shaped light curves, but each contain a slight difference in peak luminosity (because they are not perfect standard candles). It was the observation of this disparity in peak luminosities that led to the discovery of the first photometric correction and thus began SNe Ia standardisation.

2.2 Empirical Photometric Corrections

The usefulness of SNe Ia as standard candles was questioned when it was shown that the natural dispersion in their luminosities was statistically significant and could be impacting the accuracy of cosmological parameters (e.g., Phillips, 1993; Hamuy et al., 1995). Therefore, a way to limit this dispersion needed to be found. Analysis of SNe Ia light curves, derived from photometry (see Section 2.1), was the inspiration for the vital process of SNe Ia standardisation used today to improve cosmological analysis.

A relationship between the width of a SNe Ia light curve and luminosity was first identified by Phillips (1993) who showed that SNe Ia light curves that fall more rapidly have lower peak luminosities. In other words, intrinsically brighter SNe Ia have wider light curves. These findings were further reinforced by Hamuy et al. (1995). This observation revealed an opportunity to 'correct' SNe Ia luminosities based on their light curve shapes (by taking this relationship into account when calculating luminosities). A similar relationship between the light curve colour and luminosity was later identified by Riess et al. (1996) where it was found that brighter SNe Ia were on average more blue in colour.

These two corrections were more rigorously formalised by Tripp (1998) who showed that the addition of two linear parameters, that corrected for the relationships light curve width and colour had with luminosity, to the calculation for standard brightness, allowed the scatter of the SN Ia sample could be lowered to $\sim$0.15 mag (down from $\sim$0.35 mag). The lower the scatter, the more accurate the measurement of the standard brightness and hence distances for cosmology. This success led to further investigations and the method was further refined (e.g., Guy et al., 2007; Betoule et al., 2014) by employing an algorithm known as SALT (spectral adaptive light-curve template) to fit the SN Ia light curve and estimate parameters for colour and width.

To demonstrate the application of this empirical two-parameter standardisation method we first start with the equation to calculate the distance modulus,

$$\mu = m_b - M_0 \tag{2}$$

where m_b is the observed apparent magnitude (where magnitude describes brightness) and M_0 the standard absolute magnitude. The parameter μ is the distance modulus and is a way of expressing distances in astronomy on a logarithmic scale using magnitudes. True distances can subsequently be derived using a rearranged form of Eq. 1 mentioned earlier:

$$\mu = 5\log_{10}(d) - 5 \tag{3}$$

where d is the distance in parsecs. Eq. 2 holds true for all standard candles. However, when using standardisable candles like SNe Ia, the value of M_0 is not truly constant for different

objects. We therefore use a refined version of Eq. 2 when referring to SNe Ia distance moduli:

$$\mu_{data} = m_b - M_{cor} \tag{4}$$

where μ_{data} is the standardised distance modulus of a SN Ia in a sample and M_{cor} is the absolute magnitude that has been corrected by the empirical standardisation corrections for stretch and colour. As suggested by the previous discussion, M_{cor} can be expressed by the form,

$$M_{cor} = M - \alpha x_1 + \beta c \tag{5}$$

where M is the average absolute magnitude before standardisation and α and β are the empirical linear standardisation coefficients that correct for the SNe Ia light curve stretch (x_1) and colour (c). 'Stretch' is an analogous term for the light curve width and is used commonly today to apply the correction discovered by Phillips (1993). x_1 and c are parameters provided by the light curve fitting algorithm (e.g., SALT - Guy et al., 2007). Combing Eqs. 4 and 5 yields the full expression for the standardised distance modulus first suggested by Tripp (1998):

$$\mu_{data} = m_b - M + \alpha x_1 - \beta c \tag{6}$$

If the SNe Ia data was a perfect match to cosmology models, then one would expect to find $\mu_{data} = \mu_{cosmo}$, where μ_{cosmo} is calculated using a standard cosmology model (see Section 3 for more on how this is accomplished). Therefore, to see how well state-of-the-art models match the data, 'Hubble residuals' can be calculated according to the expression:

$$\Delta\mu = \mu_{data} - \mu_{cosmo} = m_b - M - \mu_{cosmo} + \alpha x_1 - \beta c \tag{7}$$

where $\Delta\mu$ denotes standardised Hubble residuals. The scatter of $\Delta\mu$ about zero tells us how well cosmology models match observations. Comparison to cosmology models is best done through the use of a Hubble Diagram which will be discussed further in Section 2.3. The aim of SNe Ia standardisation is to lower this scatter to an extent that is sufficient to allow SNe Ia data to be used reliably in distance calculations. The average of all M_{cor} values calculated for a sample of SNe Ia using Eq. 5 can be used to replace M_0 in Eq. 2 meaning SNe Ia can be treated as standard candles. This means distance moduli can be calculated for any SNe Ia by using just a measurement of m_b, provided the value of M_0 is reliable. Therefore, it is extremely important to find ways to limit the scatter in M_{cor} values in a SNe Ia sample as this leads to a more accurate and constrained average M_0 value.

Hubble residuals are also useful for obtaining evidence for the existence of a third correction coefficient, γ. Plotting Hubble residuals (where μ_{data} is corrected using just α and β using Eq. 6) against a property of the host galaxy such as mass or colour (see Section 4.3 for more) reveals that the SNe Ia lie within two distinct populations. SNe Ia from more massive host galaxies are on average brighter, after standardisation, than those from low mass hosts (Kelly et al., 2010; Sullivan et al., 2010). This is generally parameterised as a step function and is known in the literature as the "host-step" correction. This extra correction is an essential part of most SNe Ia analyses today (e.g., Brout et al., 2022), even though its origin is still not fully understood and is an area of ongoing research (e.g., Wiseman et al., 2023; Chung et al., 2024). Although the original host-step correction uses the environmental property host galaxy mass, other environmental tracers have also been used with varying success (e.g., Kim et al., 2018; Briday et al., 2022). Examples include global host galaxy colour, local colour and local mass (discussed further in Section 4.3). A plot of corrected Hubble residuals against a valid environmental tracer should result in two visible SNe Ia populations to which a step function can be fitted. The updated version of Eq. 6 that includes the host-step correction is,

$$\mu_{data} = m_b - M + \alpha x_1 - \beta c + \gamma p \tag{8}$$

where γ is the value of the host step (the magnitude difference between the upper and lower step of the fitted step function). With,

$$p = \begin{cases} 1, & \text{if tracer value} > \text{breakpoint}, \\ 0, & \text{otherwise} \end{cases} \tag{9}$$

which means that the gamma correction is only applied to SNe Ia from one population (so that the two distinct populations 'merge' into one with a consistent average brightness). Using Eq. 8, the Hubble residuals expression becomes:

$$\Delta\mu = \mu_{data} - \mu_{cosmo} = m_b - M - \mu_{cosmo} + \alpha x_1 - \beta c + p\gamma \tag{10}$$

Eqs. 8 and 10 are the main forms of the photometric standardisation equations that are used in this investigation. The α, β and γ terms each add a small correction to M so that the scatter of the overall SNe Ia population in the sample is reduced. A lower scatter means a more accurate value of absolute magnitude can be calculated and therefore, an improved distance measurement. The effectiveness of this equation is dependent on the accuracy of the α, β and γ values used.

Therefore, improving the accuracy of α, β and γ is a vital aspect of SNe Ia standardisation and is an area of active research (e.g.,Rose et al., 2020; Ginolin et al., 2025a,b). There are no 'true' values for α, β and γ as they are all found empirically from SNe Ia data. Instead, 'best' values can be derived and applied to the SNe Ia sample to reduce dispersion. Best values are hard to find due to the underlying relationships between variables and uncertainties. For more on the different ways α, β and γ can be calculated and how uncertainties are included for a given sample of SNe Ia, see Section 4. Although the use of α, β and γ corrections has been shown to effectively reduce SNe Ia dispersion, it is important to find more ways to improve this process to aid cosmology. This is because, as discussed in Section 1, these empirical photometric corrections are not fully understood and may not directly correct for the root causes of the SNe Ia luminosity dispersion. One way to do this is to introduce new spectroscopic correction terms into the standardisation procedure, which is discussed in Section 6.

2.3 Latest Findings in SNe Ia Standardisation and Cosmology

As discussed in Section 2.2, current SNe Ia standardisation methods employ additional terms, as seen in Eq. 8, that correct SNe Ia luminosities. These corrections alter the luminosity of each SNe Ia in a sample such that the overall average dispersion of the sample is lowered. This yields a more accurate value of the standard brightness which is used to calibrate more accurate distance measurements, meaning cosmological parameters can be constrained further. This process depends on the accuracy of the correction coefficients α, β and γ. The best known up-to-date values of α, β and γ from different recent investigations and how effectively they standardise a sample of SNe Ia will be discussed below.

The same ZTF data used in this investigation (see Section 3 for data) was also studied by Ginolin et al. (2025a,b). These authors used a total χ^2 minimisation routine and simultaneous fits to acquire precise values of α, β and γ for a volume limited sample (VLS) of 938 SNe Ia objects (see Section 3 for more on VLSs and fitting routines). By using local colour as the environmental tracer for the γ coefficient, values of α = 0.161$\pm$0.010, β = 3.05$\pm$0.060 and γ = 0.143$\pm$0.025 were obtained. (Some studies present values of α, β and γ with negative signs depending on how Eq. 7 is defined. For this report, all values of α, β and γ stated will be positive to maintain consistency). Rigault et al. (2025) then showed that using these values to correct the luminosities of a large sample of $>$2000 SNe Ia, allowed the luminosity dispersion

to be successfully reduced from a scatter of 0.33 mag to ∼0.15 mag using normalised median absolute deviation as a suitable scatter estimator.

Rigault et al. (2025) also used their standardised sample to create a Hubble diagram which is shown in Fig. 2. Hubble diagrams are a vital part of cosmological analysis as they are used to compare the behaviour of standardised SNe Ia samples to cosmological models. They are produced by plotting μ_{data} (from Eq. 8) or $\Delta\mu$ (from Eq. 10) against redshift z and a cosmological model (μ_{cosmo}) can be overlaid for comparison. Hubble diagrams will be a core part of this investigation so Fig. 2 is provided as an example from the literature for reference.

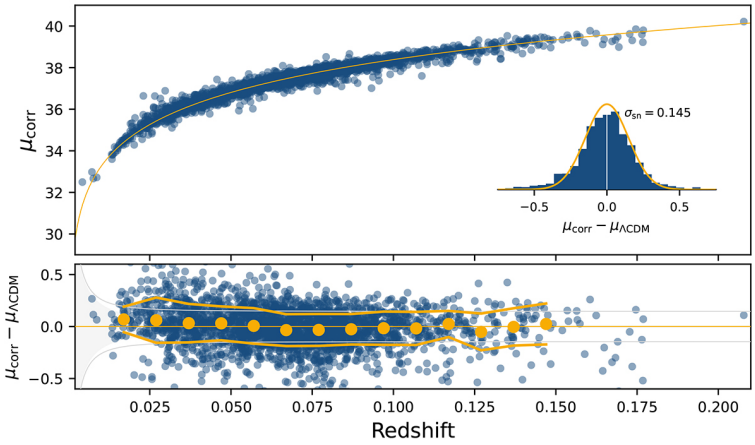

Figure 2: Example Hubble diagram taken from Rigault et al. (2025) to show how well photometric SNe Ia standardisation methods, using state-of-the-art data, are performing currently. TOP: Corrected distance moduli for 2629 non peculiar SNe Ia against redshift. Yellow line is a comparison to the ΛCDM cosmology model anchored on the Planck Collaboration (2020). BOTTOM: Standardised Hubble residuals against redshift. The scatter in the diagram is $\sim$ 0.15 mag which is in good agreement with other literature and sets the current benchmark for SNe Ia standardisation.

A dispersion of $\sim$ 0.15 mag, after standardisation, achieved by Rigault et al. (2025) is consistent with other state-of-the-art results in the literature such as those found in the Pantheon+ analysis (Brout et al., 2022). Their study used 1701 light curves from 1550 unique SNe Ia from 18 different publicly available and privately released samples to constrain cosmological parameters. They showed that their constraining power was improved by a factor of 2 and, for a flat ΛCDM model, a value of Ω_m = 0.334$\pm$0.018 was determined. This tells us that matter (baryonic or dark) accounts for only ∼30% of the total energy in the universe. For a flat $\omega_o CDM$ model they obtained values of ω_0 = -0.90$\pm$0.14 and H_0 = 73.5$\pm$1.1 km s^{-1} Mpc^{-1}. This ω_0 value is close to -1 which is to be expected if the expansion of the universe is caused by a cosmological constant Λ. This provides more insight into the nature of dark energy. However, other studies such as the DESI Collaboration (2025) show that ω might not = -1 at the $\sim 2\sigma$ level, further highlighting inconsistencies that currently exist in cosmology.

The luminosity scatter in the sample used by Brout et al. (2022) was also shown to reduce to $\sim$ 0.15 after standardisation, when not taking into account objects with a scatter potentially induced by peculiar velocities. The values of the standardisation parameters obtained for their most successful model were α = 0.148$\pm$0.004 and β = 3.09$\pm$0.04. An important part of this study to note is that γ was found to be $\approx$ 0 due to the fact that most of its correction was already taken into account and was absorbed by the more complex bias correction term used by their model. See Brout et al. (2022) for more on the model and bias corrections used.

Other studies on smaller samples of SNe Ia have also found similar values (within 1σ) for α, β and γ to the two studies mentioned above. For example, Rose et al. (2021) used 103 SNe Ia from the Sloan Digital Sky Survey along with a simultaneous fit that employed a Bayesian hierarchical model called UNITY to obtain α = 0.170$\pm$0.018, β = 3.2$\pm$0.2 and γ = 0.11$\pm$0.03. (where γ in this case was found using host mass as the environmental tracer). These values reduced the unexplained scatter in their sample from $0.122^{+0.019}_{-0.018}$ mag to 0.114$\pm$0.016 mag which is consistent with other results in the literature. However, this means there is still a certain amount of scatter in their sample that is unexplained.

The studies mentioned above highlight the current state of SNe Ia standardisation. At present, most studies employ photometric standardisation methods that effectively reduce luminosity scatter to the benchmark value of $\sim$ 0.15 mag suggested by Tripp (1998). In most recent studies the approximate values of the correction parameters are found to be: $\alpha \approx 0.15$, $\beta \approx 3$ and $\gamma \approx 0.1$. However, the exact values of α, β and γ depend greatly on the SNe Ia sample used, as well as the complexity and type of standardisation model or fitting routine applied. A scatter of $\sim$ 0.15 mag is sufficient to constrain cosmological parameters to a certain extent, as shown by Brout et al. (2022), but there is still room for improvement. For example, to obtain more convincing evidence for a cosmological constant, the value of ω_0 found by Brout et al. (2022) could be constrained further to see if it truly lies near -1. Furthermore, most studies also show that there is still a significant amount of scatter left in their samples that is not taken into account by their models and cannot be justified by measurement error alone (e.g., Rose et al., 2021). This can be parameterised as intrinsic dispersion σ_{int} and will be discussed further in Sections 3 and 4. This means there is still room for improvement in the field of SNe Ia standardisation as there must still be underlying causes for dispersion that are not being corrected for by current methods. If these improvements can be shown to significantly reduce SNe Ia luminosity scatter, it will allow cosmological parameters to be constrained even further, which is vital for our understanding of the universe.

3. Data Acquisition & Analytical Procedures

This investigation uses data from the ZTF SN Ia DR2 sample presented in Rigault et al. (2025). The initial dataset contains 3628 spectroscopically confirmed SNe Ia, which is lowered to a sample of 2663 after basic data cuts are made (see Section 3.2). This is still the largest collection of well-sampled SNe Ia across any redshift range to date. This provides an incredible opportunity to investigate deeper into SNe Ia standardisation than ever before. A brief overview on how the data was collected and what the DR2 dataset contains is provided in Section 3.1. The basic data cuts made to improve the quality of the sample are outlined in Section 3.2. Smaller sub-samples from the full DR2 sample that were used in this investigation are described in Section 3.3. Finally, data analysis methods that were used throughout this investigation are discussed in Section 3.4.

3.1 ZTF SN Ia DR2 Dataset

The Zwicky Transient Facility (ZTF), named after astronomer Fritz Zwicky, is a wide-field sky astronomical survey located in California (see Bellm et al., 2018 for more details). The facility uses a 576 megapixel camera, mounted to the P48 Schmidt telescope at the Mount Palomar Observatory (Dekany et al., 2020). It has detected thousands of SNe a year since it began operations in March 2018. The DR2 dataset contains 3628 SNe Ia that were detected and classified by the ZTF up to the end of December 2020. For each SNe Ia, the full DR2 dataset contains: A unique identifier known as 'ztfname'; redshift z; time of peak brightness (for nebula

spectroscopy) t_0; the stretch parameter x_1; colour c; and a parameter x_0 used to calculate m_b via the equation:

$$m_b = -2.5\log_{10}(x_0) + c \tag{11}$$

where c is a constant set to 10.652 in this investigation. The dataset also contains absolute errors and covariances associated with each parameter. The recent recalibration of the SALT light curve fitter from Guy et al. (2007); Betoule et al. (2014), retrained by Taylor et al. (2021) as SALT2.4 was used to obtain parameters such as x_1, c, t_0 and their uncertainties. The SALT fits were performed in the phase range $\phi \in [-10, +40]$ days, an interval over which the algorithm is sufficiently trained. Another parameter the SALT algorithm provides for the DR2 data set is 'fitprob'. This is a quality of fit parameter derived from the χ^2 statistic. This will be useful for making quality cuts in the data, discussed in the next section.

3.2 Basic Data Cuts

As suggested by Rigault et al. (2025), certain basic quality cuts should be made to the DR2 dataset to ensure the derived parameters (such as α, β and γ) are reasonable for use in cosmological analysis. The recommended cuts, which were applied in this investigation, are detailed in Table 1:

Cuts	n targets	removed	% removed
Master list	3795	–	–
+ ZTF light curve	3778	17	0.4
+ a spectrum	3668	110	2.9
+ confirmed "Ia"	**3628**	40	1.1
Basic cuts			
Good light curve sampling	2960	668	18.4
$x_1 \in [-3, +3]$	2899	61	2.1
$c \in [-0.2, 0.8]$	2861	38	1.4
$\sigma_{t_0} \leq 1$	2836	25	0.9
$\sigma_{x_1} \leq 1$	2822	14	0.5
$\sigma_c \leq 0.1$	2809	13	0.4
"fitprob" $\geq 10^{-7}$	**2667**	142	5.1

Table 1: Basic data quality cuts that were applied to the ZTF SNe Ia DR2 dataset in this investigation, as recommended by the literature. Table taken from Rigault et al. (2025).

As shown in Table 1 the basic quality cuts reduce the sample size down to 2667 SNe Ia. The cut 'good light curve sampling' means the only objects included in the final sample were those with light curves that had (i) at least seven 5σ flux detections within the rest frame phase range ϕ (see section 3.1), (ii) at least two detections at pre and post-maximum (where the maximum is at time t_0) and, (iii) detections in at least two bands. The cut applied to c is recommended to be less stringent than that used in other literature (e.g., Rose et al., 2022) to allow a larger sample size. Ginolin et al. (2025b) have shown that only considering objects with $c < 0.3$ (the usual cut in the literature) has no significant impact on the results. Therefore, the c cut shown in Table 1 is preferred because it provides a larger sample size to use, which means that it is more representative and the results may be more reliable. The other cuts detailed in Table 1 limit the range of x_1 values as per the recommendation by Rigault et al. (2025), include values of t_0, x_1 and c that are known with a good precision (e.g. $\sigma_{t_0} \leq 1$) and, a large enough 'fitprob' from the SALT algorithm.

A further cut can be made to remove 'peculiar objects' (e.g. those with a subclass such as

'Ia-csm' or '91bg-like') which reduces the sample size to 2169. This sample is the final version of the dataset that was used throughout this investigation. Other subsets can then be taken from this sample for different analyses, which will be discussed in the next section.

3.3 Volume Limited and Spectroscopic Samples

The full DR2 sample used in this investigation contains 2169 objects, after applying the basic data quality cuts discussed in Section 3.2 (henceforth DR2cut). Rigault et al. (2025) showed that by only including objects with a redshift $z < 0.06$, the first of two new subsets used in this investigation can be created. This is known as the 'Volume Limited Sample' (henceforth VLS) because a cut in redshift is essentially a cut in distance, meaning objects in this sample are within a certain sphere of volume around us. The VLS used in this investigation contains 909 SNe Ia after removing all objects with $z > 0.06$ from DR2cut. This sample is shown to be free from significant non-random selection functions by Amenouche et al. (2025). This makes the VLS extremely useful for this investigation because the observed distributions of any parameter (such as x_1, c, x_0 etc.) are representative of the 'true' underlying distribution. This is because this sample is free from Malmquist bias, which is the effect caused by the preferential detection of intrinsically bright objects. See Section 5 for a more detailed discussion on bias. The VLS is therefore the main sample used for the investigation detailed in Section 4 as it negates the need to include complex bias corrections. The VLS was also extensively studied by Ginolin et al. (2025a,b), which provides a great opportunity to compare some of the results of this investigation with the latest state-of-the-art research.

The second subset of objects created for this investigation consists of objects for which spectroscopic data from the ZTF is available. Spectroscopic data is needed for this investigation because the primary objective is to demonstrate that using corrections derived from the spectroscopic data of SNe Ia could improve upon current photometric standardisation. The spectroscopic data in question is from Burgaz et al. (2025) where the velocities and pseudo-equivalent widths (pEW) of a key SNe Ia spectral feature was investigated. The spectral feature used was the silicon feature (Si II) at λ6355 Å in the spectra of SNe Ia. Section 6 will go into more detail on the definition of pEW and how possible new corrections could be derived from this data. Section 7 will then discuss if these spectroscopic corrections can improve upon the current photometric corrections. The number of objects from DR2cut for which spectroscopic data from Burgaz et al. (2025) is available is 416. This is the spectroscopic sample used in this investigation, which is henceforth referred to as the 'spectroscopic data available' (SDA) sample.

It is important to note that the SDA sample also only contains objects with $z < 0.06$. Therefore, it could be argued that the SDA sample is a representative subset of the VLS. However, this may only be true if the objects that make up the SDA sample were drawn from the VLS at random. This raises an important question: Is the SDA sample free from bias? As discussed in Section 2.1, spectroscopy requires a lot of light. Therefore, the SDA sample may suffer from a selection bias towards brighter objects, similar to that found in DR2cut. This issue is further investigated in Section 5, as the presence of Malmquist bias in the SDA sample may affect the validity of the results of this investigation if it is not taken into account.

3.4 Data Analysis Methods

An overview of the data analysis techniques used in this investigation is provided in this section to allow a better understanding of how the results, and the conclusions they reveal, were obtained. The bulk of the investigative work for this project was carried out by using computer programs written using Python code. Packages such as 'matplotlib' and 'astropy' were used to

plot graphs and implement cosmology models.

3.4.1 Comparing Standardisation Methods Using Intrinsic Dispersion

The goal of the project was to determine whether SNe Ia standardisation could be improved by implementing new corrections derived from spectroscopic data. In order to see how well a particular approach standardises a sample of SNe Ia, a robust method is needed to compare the dispersion of the sample, for each different standardisation method employed. To achieve this, Hubble Diagrams (seen in Fig. 2) can be plotted from the data. Then, this can be compared to a standard model. For example, a plot of μ_{data} against z can be compared to the standard flat cosmology model ΛCDM by plotting the distance modulus derived using this model (μ_{CDM}) against z on the same plot. In this work, the values of μ_{CDM} were obtained by a Python program that used the package "astropy.cosmology.Planck18" (Astropy Collaboration et al., 2013; Price-Whelan et al., 2018), which applies cosmological parameters of $H_0 = 67.66\,\mathrm{km\,s^{-1}\,Mpc^{-1}}$ and $\Omega_m = 0.30966$, to calculate distance modulus values for given values of redshift. Furthermore, the μ_{CDM} values can then used to calculate Hubble residuals (Eq. 10) which can also be plotted against z as seen in Fig. 2. The model that residuals are compared to is the line of y = 0. This is because, as discussed in Section 2.2, a perfect result would result in $\mu_{data} = \mu_{cosmo}$ and the residuals being equal to zero. We are assessing how well the model matches the data by seeing how the residuals, $\Delta\mu$, are distributed around zero. To compare how well these models match the data, this investigation made use of the χ^2_{red} statistic. This is a statistical 'goodness of fit' measure and is calculated by,

$$\chi^2 = \sum_i \left(\frac{\text{model}_i - \text{data}_i}{\text{uncertainty}_i} \right)^2 \tag{12}$$

$$\Rightarrow \chi^2_{red} = \chi^2/dof \tag{13}$$

where dof is the degrees of freedom. The closer the value of χ^2_{red} is to 1, the better the fit of the model to the data. In general, the SNe Ia data is never a perfect match to the model because, even after standardisation, there exists a certain intrinsic dispersion that has not been corrected for within the sample. The intrinsic dispersion can be thought of as the amount of scatter left in a sample that still needs to be corrected for. In theory, a perfect standardisation process would yield a χ^2_{red} value of 1. However, it is impossible to account for all the causes of dispersion in a SNe Ia sample because we cannot get direct measurements of every single atom in a SNe Ia progenitor system. Instead, general corrections must be made to try and lower the dispersion as much as possible. This means the χ^2_{red} score cannot equal 1 through the position of the data alone. Instead, the only way to achieve a 'perfect' χ^2_{red} value of 1 is to alter the uncertainty term in the denominator in Eq. 12. This means the intrinsic dispersion can be estimated as an extra term in the uncertainty (σ_{int}) that is added in quadrature. The value of σ_{int} is such that it increases the size of the uncertainty in the χ^2 calculation (Eq. 12), so that the final value of χ^2_{red} is approximately 1. In other words, σ_{int} is a parameterisation of the amount of scatter leftover in the sample that has not been corrected for by SNe Ia standardisation. The main aim of SNe Ia standardisation today is to decrease σ_{int} as much as possible by finding more accurate or new corrections that account for a deeper root cause of dispersion. This report focuses on the latter by investigating spectroscopic data as a source for new corrections.

Using Python code, an algorithm was programmed for this investigation that estimated a value of σ_{int} (and its uncertainty) for any given standardised SNe Ia sample. If a certain standardisation method resulted in a lower value of σ_{int} than another method (for the same SNe Ia sample), then it provides evidence for that method being more optimal. This is the main way in which the effectiveness of different standardisation methods were compared in this investigation. The algorithm first calculates the base error (error caused by measurement uncertainty

in parameters such as x_1, c, m_b etc.) in μ_{data} for each SNe Ia in a sample after standardisation. Then, a value of σ_{int} can be added to this in quadrature. The χ^2_{red} statistic is calculated between the data (e.g. $\Delta\mu$) and the model (e.g. y = 0) for this value of σ_{int} and stored. The algorithm loops through a set of possible values of σ_{int} and returns the best value that yields a χ^2_{red} closest to 1. The uncertainty is estimated as the range of values of σ_{int} that yield a χ^2_{red} value close to 1, within a 1σ (68% confidence) interval. This best value is used as the estimate for σ_{int} for the particular standardisation process used on that sample. The equations used to calculate the base error in μ_{data} are discussed in more detail in Section 3.4.2.

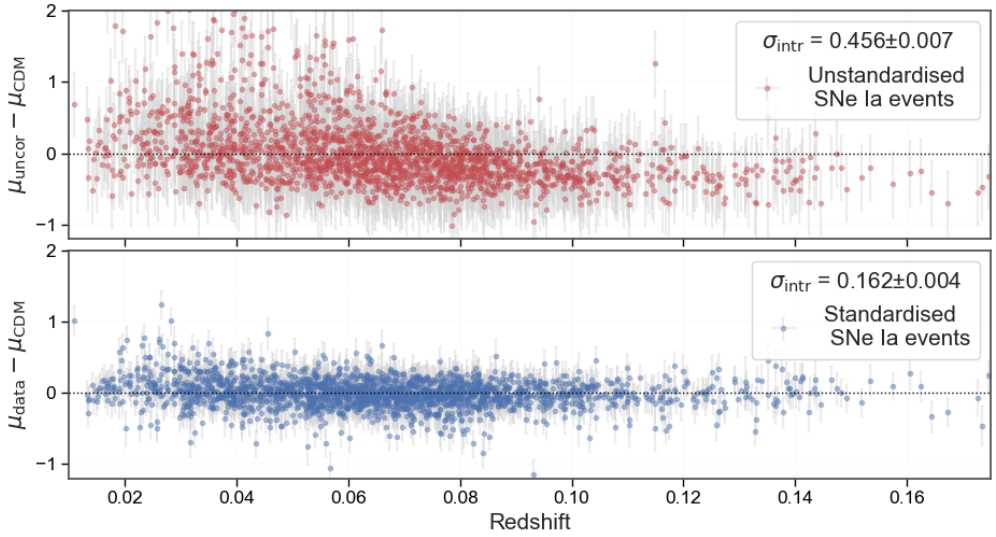

Figure 3: Hubble residuals before (TOP) and after (BOTTOM) standardisation to demonstrate how the estimate for σ_{int} decreases when the sample is standardised. Better standardisation will therefore further reduce σ_{int}. The SNe Ia sample used for this example is DR2cut (see Section 3.3) and is standardised using the light-curve stretch, light-curve colour, and host step photometric corrections. The correction parameters used for this were α = 0.161, β = 3.05 and γ = 0.143 from Ginolin et al. (2025a,b). The γ correction uses local colour as the environmental tracer and the step function is applied at the standard literature cut of local $(g-z)$ = 1 mag.

To further demonstrate the intrinsic dispersion method, Fig. 3 shows a plot of residuals against redshift before and after standardisation. As can be seen, the intrinsic dispersion is significantly lowered after applying the usual photometric corrections, using the values of α, β and γ from Ginolin et al. (2025a,b) (see Section 2.3) to standardise the DR2cut sample. Using these state-of-the-art standardisation parameters and the intrinsic dispersion estimation algorithm yields an estimate of σ_{int} = 0.162 mag. This is close to the expected value of $\sim$0.15 mag from the literature. The algorithm could be over-estimating σ_{int} in this investigation due simplification assumptions made when calculating the base error in μ_{data}. This is discussed further in Section 3.4.2. A larger σ_{int} could also be caused by outliers in the sample, several of which can be seen in Fig. 3. Therefore overall, Fig. 3 shows that the intrinsic dispersion method is a robust way to measure how well a sample is being standardised for this investigation. Any over-estimations do not impact comparisons between different methods within this investigation itself. Further improvements must be made to refine the σ_{int} estimation process in future investigations so that it is more agreeable with the literature.

3.4.2 Error Calculations

The error on μ_{data} can be approximated by applying the general rule of combination of uncertainties to Eq. 8:

$$\sigma^2_{\mu_{data}} = \sigma^2_{m_b} + (\alpha\sigma_{x_1})^2 + (x_1\sigma_\alpha)^2 + (\beta\sigma_c)^2 + (c\sigma_\beta)^2 + (p\sigma_\gamma)^2 + \sigma^2_{int} \quad (14)$$

where σ_x denotes the absolute error for a given variable x. Note that the terms $(\gamma\sigma_p)^2$ or $(\sigma_M)^2$ do not appear in this approximation because p takes fixed values (of 1 or 0) and M is the average unstandardised brightness of the sample is therefore treated as a fixed parameter. σ_{int} is the intrinsic dispersion as discussed in Section 3.4.1.

The approximation in Eq. 12 treats the parameters α, β and γ as if they were free parameters with uncertainties, like x_1, c or m_b, that affect each individual SNe Ia. It also assumes that they are uncorrelated. In reality α, β and γ are global nuisance parameters determined from global fits (see Section 4). This means Eq. 12 is not technically appropriate to use when calculating the error in μ_{data} for each individual supernova. This is because it includes terms with σ_α, σ_β and σ_γ and does not take covariances between parameters into account. This leads to an inflation in the error bars, and therefore the prediction for σ_{int} is underestimated.

Alternatively, an equation suggested by Kessler and Scolnic (2017) is more appropriate:

$$\begin{aligned} \sigma^2_\mu &= \sigma^2_{int} + (\sigma^z_\mu)^2 \\ &+ C_{m_b,m_b} + \alpha^2 C_{x_1,x_1} + \beta^2 C_{c,c} \\ &+ 2\alpha C_{m_b,x_1} - 2\beta C_{m_b,c} - 2\alpha\beta C_{x_1,c} \end{aligned} \quad (15)$$

where $C_{x,y}$ represents the covariance between parameters x and y. The covariance of the same parameter is equal to the square of the absolute error (e.g $C_{m_b,m_b} = (\sigma_{m_b})^2$). Eq. 13 is therefore very similar to the approximation in Eq. 12 but it incorporates covariance terms and treats α, β and γ as fixed. This is the preferred method and was the equation used to calculate the error in μ_{data} throughout this investigation (including the algorithm to find σ_{int} discussed in Section 3.4.1). It is important to note that the $(\sigma^z_\mu)^2$ term, which is the error on μ caused by the uncertainty in peculiar velocity and redshift measurements, is very small and was treated as zero for the purpose of this investigation. This could lead to the values of σ_{int} obtained by the algorithm discussed in Section 3.4.1 being slightly overestimated because the base error is too small.

3.4.3 Using Global Fits to Determine Standardisation Parameters

Section 4 considers the photometric standardisation parameters α, β and γ that were obtained in this investigation for the VLS (see Section 3.3) and compares how well they standardise the sample using the intrinsic dispersion method discussed in Section 3.4.1. Similarly, Section 6 uses spectroscopic data to find evidence for new spectroscopic standardisation corrections. The different methods used to determine these standardisation parameters throughout Sections 4 and 6 are discussed here, to fully establish and clarify the processes used.

Firstly, standardisation parameters are found via a process called independent fitting. This is where uncorrected residuals $\Delta\mu$ are plotted against a parameter that needs to be corrected for (e.g. light curve stretch x_1, light curve colour c or an environmental tracer). Uncorrected residuals can be obtained by simply using Eq. 10 with α, β and γ set to zero (because we do not know what their values are yet). The resulting plot shows the relationship between the residuals and that parameter. For example, a plot of residuals against x_1 suggests the relationship resembles a negatively sloped linear function. The gradient of the line of best fit of this

relationship can be used as an estimate of the value of α. This is because for the independent fitting process, we assume that x_1, c and environmental tracers (and by extension α, β and γ) are independent of each other. This means, for example, that we assume the plot of $\Delta\mu$ against x_1 has the form $y = mx + c$ like an ordinary linear function. Of course, y here is the dependent variable $\Delta\mu$, x is the independent variable x_1 and, m is the gradient α (because α and x_1 are multiplied together in Eq. 10). The other terms in Eq. 10 are treated to be part of the constant c because we are assuming an independency of variables. Section 4 considers in more detail whether or not this assumption is valid. Python programs were written to produce independent fits between residuals and photometric or spectroscopic data from the SNe Ia to derive correction parameters. Packages such as 'scipy.optimize.curve_fit' were used to fit model functions to these plots to obtain the values of the standardisation parameters. The results of this process for the VLS are presented in Section 4. Section 6 uses the SDA sample to produce independent fits for spectroscopic data variables like pEW or silicon velocity to find evidence for new corrections.

Another way in which standardisation parameters can be determined is by fitting them simultaneously using Bayesian statistics. This investigation utilised the 'emcee' package in Python to run Markov Chain Monte Carlo (MCMC) simulations that perform multi-dimensional fits across the parameter space to find all standardisation parameters simultaneously. Python functions were written to define the log likelihoods, priors and posteriors, based on the standardised residuals formula (Eq. 10). The values of standardisation parameters from the independent fits were used to estimate the expected prior ranges. The values of standardisation parameters deemed to be the best fit values according to the MCMC fitting procedure, were taken to be those that generated the the best posterior probability when used to correct the residuals and compared to the flat (y=0) model. Errors in the standardisation parameters were estimated as the standard deviations of the posterior distribution sampled by the chain for each parameter (after making sure that the chain had converged and that the distribution was reasonably well-sampled). Details on the sampler parameters (number of steps, number of walkers, etc.), the exact forms of the log priors and likelihoods that were used, and the results from the simultaneous fits for the VLS are provided in Section 4.

4. Photometric Standardisation Parameters for the Volume Limited Sample

The processes by which the typical empirical photometric standardisation parameters, α, β, and γ, can be derived are illustrated in this section. The objective of this section is to establish the optimal method to find accurate values of α, β, and γ for a given SNe Ia dataset. This is accomplished by comparing the intrinsic dispersion in the sample after applying the correction parameters derived from each method, using the algorithm discussed in Section 3.4.1. The two methods that are compared are the use of independent versus simultaneous fits to derive the standardisation parameters. Due to the presence of a selection bias towards brighter objects that is apparent in the full ZTF DR2 SNe Ia sample (see Section 5), the Volume Limited Sample (as defined in Section 3) will is used throughout this section to avoid the need to include complex bias corrections. Sections 4.1- 4.3 demonstrate the use of independent plots for fitting α, β and γ. Section 4.4 then discusses the validity of this method due to the underlying relationships between variables. The alternative method using multiple simultaneous fits is demonstrated in Section 4.5 and the effectiveness of each method is compared.

4.1 Correcting For Light Curve Colour (β)

Brighter SNe Ia are on average more blue in colour (Tripp, 1998). This relationship can be taken into account and corrected for by SNe Ia standardisation. Section 3.4.3 described the independent fitting process used to derive the correction parameters. This method will be applied to find the strongest correction parameter, β, in this section. A plot of brightness (or preferably Hubble residuals) against light curve colour shows that there is a strong positive correlation between them. This can be modelled as a linear function where the slope of the line of best fit of the fitted linear function gives an estimate for β. Fig. 4 shows an independent fit of unstandardised Hubble residuals against light-curve colour for objects from the VLS. This is the first standardisation parameter derived by the independent fitting process because it has the strongest correlation and therefore the biggest impact on the standardisation of a SNe Ia sample. Fig. 4 was developed using 'matplot.lib' in Python and made use of the package 'scipy.optimise.curve_fit' to fit the linear function. The value of β obtained from this independent fit is β = 2.942$\pm$0.043. The uncertainty here corresponds to the uncertainty in the fitted slope, as provided by the fitting routine. This is a 1.46σ significant difference to the value obtained by Ginolin et al. (2025a,b) in their investigation on the same sample (β = 3.05$\pm$0.06). Therefore, this value is not too significantly different from the expected values in the literature, but is not in excellent agreement. This value of β will be used to standardise the VLS sample so that the next standardisation parameter α can be found.

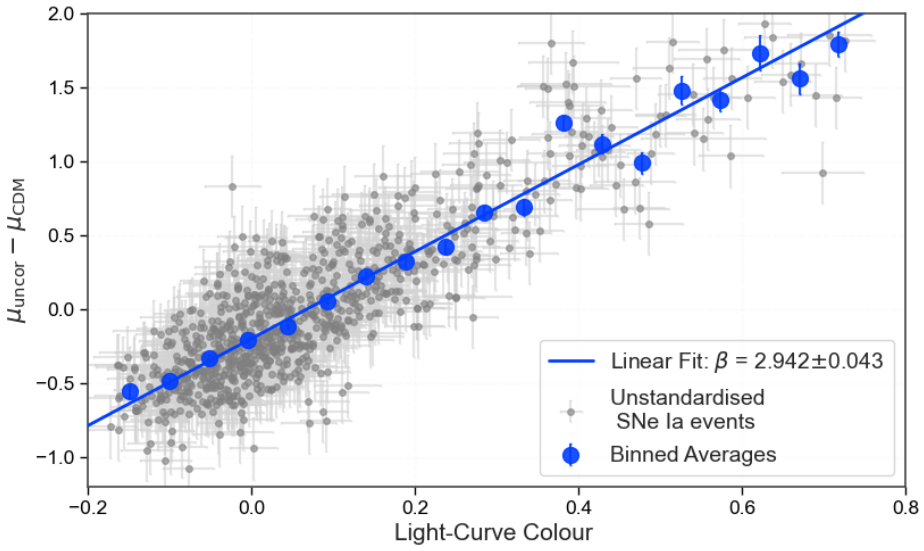

Figure 4: Independent fit of unstandardised Hubble residuals against light-curve colour for all objects from the VLS. A linear function was fitted to the data using the Python package 'scipy.optimise.curve_fit' to estimate a value of the standardisation parameter β. Binned averages have been added to help visualise the relationship more clearly. There are significantly fewer objects above $c \approx 0.3$ than below, which is why the linear relationship is slightly less clear in this region due to random noise or outliers having a larger effect.

4.2 Correcting For Light Curve Stretch (α)

The VLS was standardised using the β parameter from Section 4.1 and applying it to Eq. 8. This partially standardised sample was then used to derive the next correction parameter, α. This is because doing an independent fit to find α, after already correcting for β, should mitigate some of the issues caused by underlying relationships between variables and the value

obtained for α is more accurate. The impact of these underlying relationships is discussed further in Section 4.4. Intrinsically brighter SNe Ia have been shown to have wider light curves (Phillips, 1993; Tripp, 1998). This relationship can be described by a linear function in the plot of residuals (ideally already corrected for colour) against stretch. Where stretch is a term used to describe the width of the light curve. Fig. 5 shows a negative linear correlation between Hubble residuals corrected for colour and light curve stretch for the VLS objects. The slope of the line of best fit, fitted using the Python package 'scipy.optimise.curve_fit' is an estimate for the value of α. The value of α obtained by the independent fit in Fig. 4 is α = 0.119$\pm$0.007. The negative slope is taken into account by the sign convention used in Eq. 8. The uncertainty again corresponds to the uncertainty in the slope from the Python fitting routine. This is a 3.4σ significant difference from the value obtained by Ginolin et al. (2025a,b) (α=0.161$\pm$0.01) which means that the two values are statistically significantly different. This is the first evidence that the independent fits method may not be the most reliable way to derive standardisation parameters. This will be addressed further in Section 4.4.

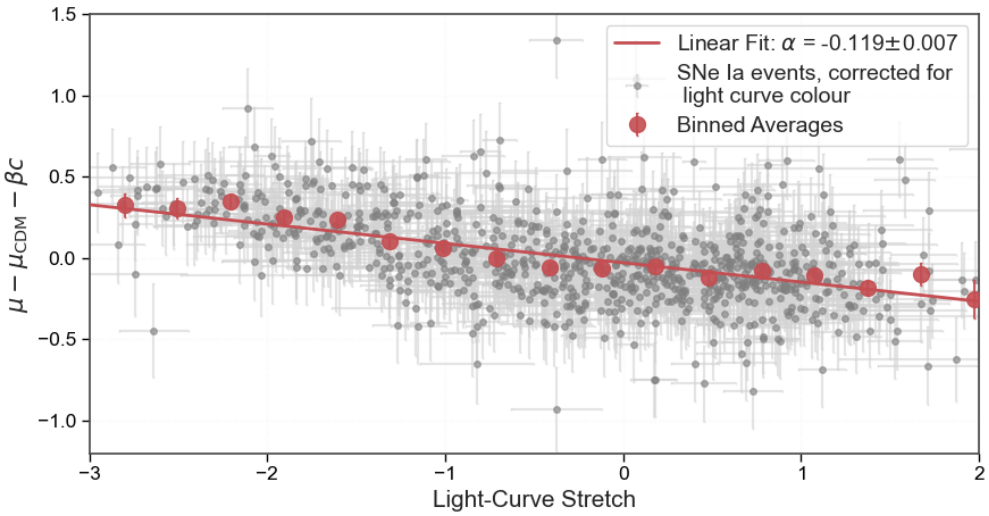

Figure 5: Independent fit of Hubble residuals (corrected for light curve colour) against light curve stretch for all objects in the VLS. A linear function was fitted to the data using the Python package 'scipy.optimise.curve_fit' to estimate a value of the standardisation parameter α. Binned averages have again been included to help visualise the relationship more clearly.

4.3 Correcting For Host Galaxy Environment (γ)

Host-step corrections have been applied using several different 'tracers' that describe the environment of the host galaxy that SNe Ia reside in (e.g. host galaxy colour, host mass, local mass, local colour, etc.). This section will focus on the global tracers host galaxy mass and host galaxy colour. Such corrections are controversial because it is not clear how they correct for root causes of dispersion because measurements from the SNe Ia themselves are not directly used. The origin of a 'host-step' correction is thus still being widely debated. This kind of correction was first discovered when it was shown that SNe Ia from higher mass host galaxies are, on average, intrinsically brighter, after stretch and colour standardisation (Sullivan et al., 2010; Kelly et al., 2010). The SNe Ia appeared to consist of two distinct populations which allows this correction to be parameterised as a step function. More recent state-of-the-art investigations have also had success applying a smooth sigmoid function instead, which matches the observed relationship better (e.g.,Ginolin et al., 2025a).

4.3.1 Host Mass Correction

After applying colour and stretch corrections, the standardised Hubble residuals generated can be plotted against host galaxy mass to reveal evidence for the host-step correction. Fig. 6 shows the results obtained for the SNe Ia in the VLS. This plot was created by defining a step function that had a y-axis value of zero before the break point, and a constant negative value after the break point. The break point therefore marks the x-axis value at which the step occurs and the magnitude of the step corresponds to γ. In Fig. 6, residuals were calculated using Eq. 10, with a value of M such that all objects below the break point had residuals that averaged to zero. All objects above the breakpoint had residuals that were on average below zero by some step. This meant the simple step-function defined could be applied to this sample. The required M value was obtained by calculating the average brightness of all objects below the standard literature break point: $\log(M_*/M_\odot) = 10$ and subtracting this as part of Eq. 10 to obtain residuals.

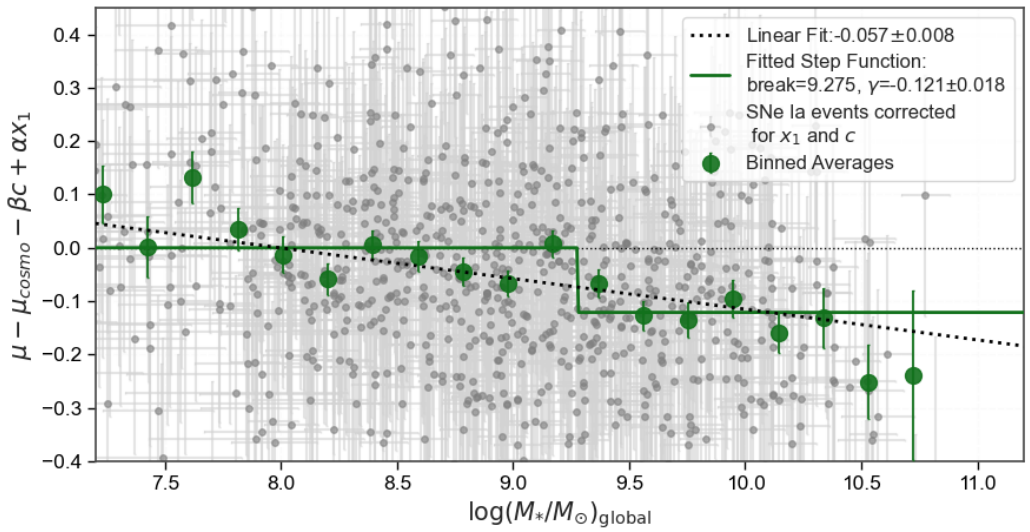

Figure 6: Independent fit of Hubble residuals (corrected for light curve colour and stretch) against host galaxy mass for all objects in the VLS. A step function was fitted to the data using a MCMC algorithm to estimate a value of the standardisation parameter γ. Binned averages have been added to help visualise the relationship more clearly. However, in this case, the binned averages highlight the fact that a step function, visually, does not suit the data well. A linear fit is also included for comparison which highlights the need for further investigation to test the goodness of fit of other models.

In order to obtain an accurate value of γ and its uncertainty, the conventional 'scipy.optimise.curve_fit' routine was not used. Instead, an MCMC algorithm was used to explore the free parameters in the step function (break-point and γ). The parameter values that provided the best posterior probability for the model were obtained from the sampler. The error was estimated as the standard deviation of the posterior distribution sampled by the chain for each parameter. It is important to note that this is still classed as an independent fitting method because it is only the parameters for the γ model that are being fitted simultaneously. The values obtained by the MCMC for the step function for Fig. 6 were: break-point = 9.277 and γ = 0.121$\pm$0.018. This break point value is slightly lower than the standard literature value of 10. The γ value is in excellent agreement with other literature values. Rose et al. (2021) obtained a mass step of γ = 0.11$\pm$0.03 which is statistically very similar (0.31σ difference) to the value in Fig. 6.

One caveat with the host mass step correction seen in Fig. 6 is that even though the value of γ obtained is in excellent agreement with other literature, visually it is hard to see how a step function is the best fit to the data when looking at the binned averages. Further investigation into this tracer should be done by comparing the goodness of fit of other models such as linear ones that might match the data better. This further highlights the inconsistencies with the host step correction and proves why it is still widely debated. This was the main motivation to investigate a second environmental tracer, such as host colour in the next section, to see if the step function form was clearer in this plot.

4.3.2 Host Colour Correction

An alternative host galaxy environmental tracer such as host colour can also be used to obtain the host step standardisation parameter, γ. This tracer was investigated due to the unconvincing shape of the data in Section 4.3.1, where the plot of residuals against host mass did not visually appear to have a strong step function shape. Using the same methods discussed in Section 4.3.1, Fig. 7 shows standardised residuals (corrected for light curve stretch and colour) against global host galaxy colour for the VLS objects. The step function can be seen more clearly in the binned averages of the data in this plot, which suggests that this tracer is more reliable. The value of γ obtained from Fig. 7 is γ = 0.108$\pm$0.010. This a 1.3σ significant difference to the value obtained by Ginolin et al. (2025a) (γ = 0.143$\pm$0.025). This means that the obtained value is not in excellent agreement with the expected values from the literature, but is not significantly different. However, it is worth noting that Ginolin et al. (2025a) used a different environmental tracer (local host galaxy colour) to derive their value. The data in Fig. 7 matches the form of a step function better, which suggests global colour is a more reliable tracer than global mass. Therefore, the value of γ obtained in this section will be favoured over the value obtained by using the global host mass tracer in the previous section.

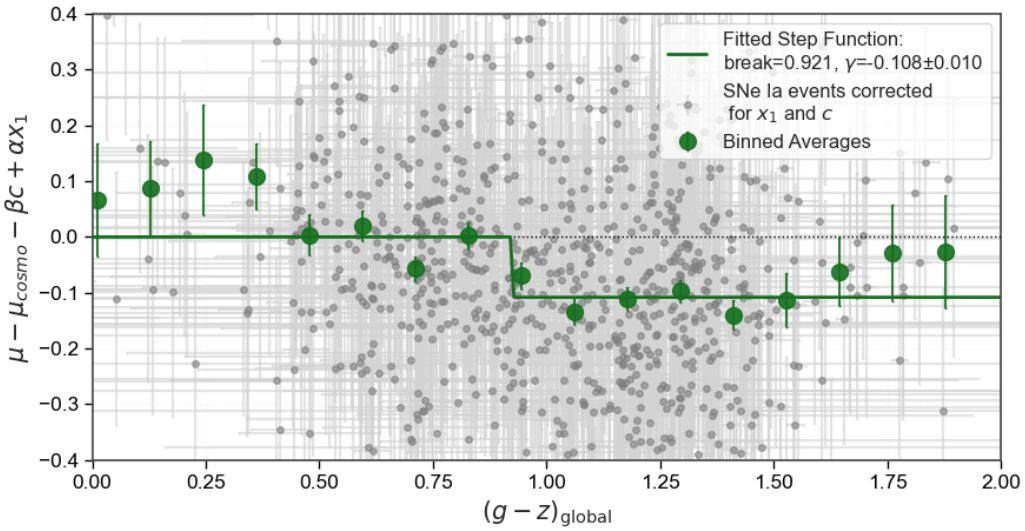

Figure 7: Independent fit of Hubble residuals (corrected for light curve colour and stretch) against host galaxy colour for all objects from the VLS. A step function was fitted to the data using a MCMC algorithm to estimate a value of the standardisation parameter γ. Binned averages have been added to help visualise the relationship more clearly. The data matches the shape of a step function in this plot better than that seen in Fig. 6, which suggests host colour is more reliable environmental tracer for deriving γ.

4.4 Are α, β and γ independent?

Sections 4.1, 4.2 and 4.3 demonstrate the use of independent fits to estimate the values of α, β and γ. These independent fits are useful because they visually display the relationships between residuals and measured SNe Ia parameters. This means the functional form of the relationship (e.g. linear, step-function etc.) is easier to identify, which is how the α, β and γ corrections were first discovered and how new corrections could also be found. Another advantage of independent fits is that they are relatively quick and simple to produce and do not require much processing power. However, the correction parameters derived from independent fits are only an estimate. This is evidenced by the fact that the values of α, β and γ derived in Sections 4.1, 4.2 and 4.3 were mostly not in excellent agreement with their expected values from the literature, but were similar.

Independent fits do not provide optimal values of correction parameters because the assumption of independency does not take underlying relationships between variables into account. Dixon (2021) highlights that "correlations between these covariates will bias estimates of the size of the corrections, as well as estimates of the variance of the final residuals". This means if parameters like x_1, c or host mass are somehow correlated, the accuracy of α, β, γ and σ_{int} is negatively impacted. To demonstrate that underlying relationships are influencing the accuracy of the independent fits, Figs. 8 and 9 recreated independent fits, but with a third variable added to the plot as a colour gradient. This will show if the third variable is impacting the relationship between the original axis variables.

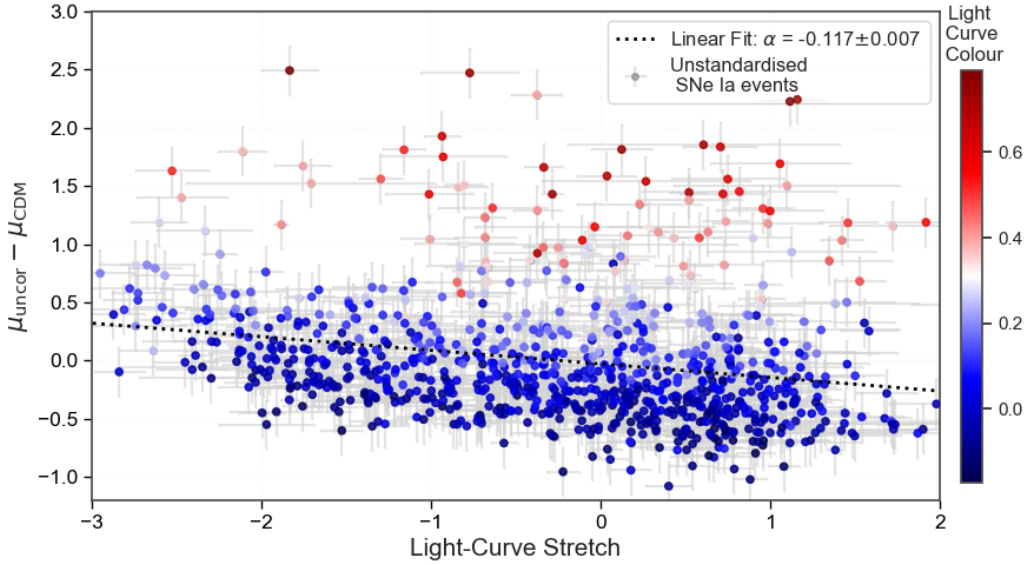

Figure 8: Unstandardised Hubble residuals against light-curve stretch for the VLS, used to derive the α correction. A third variable, light-curve colour, has been included as a colour gradient. This colour gradient shows that redder SNe Ia appear to be outliers on the plot and therefore must be corrected for by the β correction so that α can be found more accurately. This shows that there are underlying relationships between the variables and the use of independent fits may not be valid.

Fig. 8 shows the independent fit of residuals against light curve stretch, which was used to derive α in Section 4.2. However, this time the plot is created with unstandardised residuals on the y-axis (no β light curve colour correction). Light curve colour is then incorporated as a third variable using a colour gradient. A higher value of c corresponds to a redder SN Ia, and a lower

value of c means a bluer SN Ia, which is reflected by the colour-map used in Fig. 8. This plot uses unstandardised residuals because it demonstrates the fact that light-curve colour has an affect on the light-curve stretch correction more clearly. Redder SNe Ia lie further from the line of best fit in Fig. 8 and appear to be outliers, which changes the value of the slope of the fit (α). However, if a colour correction is included, as seen in Fig. 5, these outliers are brought closer to the line of best fit and α can be calculated with more confidence. However, this means the value of the β correction used has a direct impact on the value of α obtained.

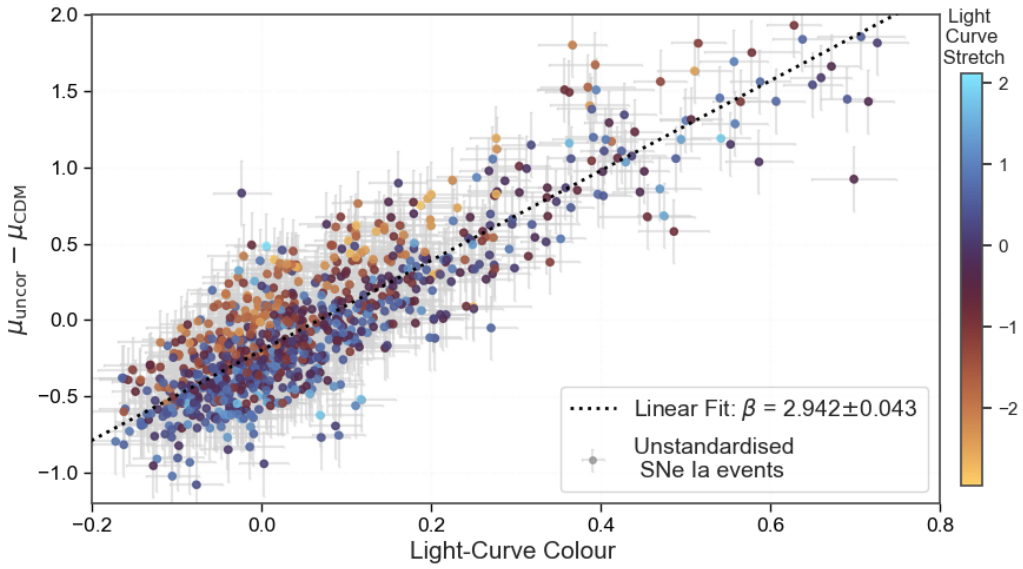

Figure 9: Unstandardised Hubble residuals against light-curve colour for the VLS, used to derive the β correction. A third variable, light-curve stretch, has been included as a colour gradient. This colour gradient shows that, on average, SNe Ia with wider light curves lie below the line of best fit. This suggests that the stretch parameter could be having an impact on the residuals-colour relationship. Therefore, β could be found more accurately by including the α correction in the residuals. This is further evidence that there are underlying relationships between the variables and the use of independent fits may not be valid.

A similar problem can be seen in Fig. 9, which is the independent fit used to derive β, but with a colour gradient depicting the distribution of light-curve stretch as a third variable included. A larger value of light curve stretch is attributed to a wider light curve. Objects with wider light curves are intrinsically brighter (Phillips, 1993). Fig. 9 shows that the majority of SNe Ia with a higher light curve stretch value (light blue objects), lie below the line of best fit. Whereas, objects with a lower stretch value (yellow-orange objects) lie, on average, above. This shows that the value of the stretch parameter could be having an impact on the position of the data in Fig. 9. This means the value of β could be found more accurately if a stretch correction is included first. However, the accuracy of α is shown to be dependent on the accuracy of β in Fig. 8 and vice versa in Fig. 9. This raises a problem: Which correction do you use first?

One solution is to start with one independent fit and use the correction it derives to find the next correction slightly more accurately. This is the method used to find α in Fig. 5. The β correction is found first because it has the strongest relationship and therefore the biggest impact. Figs. 8 and 9 also show that colour has more of an impact on the residuals-stretch relation (α) than stretch does on the residuals-colour relation (β). In theory, the α correction could then be used to go back and find β more accurately, which finds α more accurately and so on. However, this iterative process is inefficient and does not take underlying relationships

for the γ correction into account. Dixon (2021) suggest that simultaneous fits for all the parameters must be used instead, to ensure correlations between them do not introduce bias. Most studies today (e.g., Rose et al., 2021; Ginolin et al., 2025b) make use of simultaneous fitting to find more accurate standardisation parameters. Therefore, simultaneous fitting was included in this investigation and the results are discussed in the next section.

4.5 Fitting α, β and γ Simultaneously

Section 4.4 showed that independent fits are not a robust method to derive optimal values of α, β and γ because they do not take underlying relationships between variables like x_1,c or $(g-z)_{\text{global}}$ into account. Instead, the use of simultaneous fits is preferred because it does not treat parameters as independent. A combination of standardisation parameters that can minimise the intrinsic dispersion in the data is found by exploring the full joint posterior distributions of the parameters. This means underlying correlations between parameters are taken into account because when one parameter is slightly adjusted, other related parameters adapt to this change simultaneously. As discussed in Section 3.4.3, this investigation made use of an MCMC algorithm to achieve this.

32 walkers, with 5000 steps were used to explore the parameters α, β, γ and σ_{int} for the VLS simultaneously. A log likelihood was defined by using the standardised residuals model described in Eq. 10 and the uncertainty on these residuals described by Eq. 15. This meant a χ^2 statistic between the standardisation model and a set of 'target' values when plotted against redshift could be found. The set of target values were defined as $y = 0$ because a perfect standardisation leads to residuals being zero. The simultaneous fit therefore explores the free parameters α, β, γ and σ_{int} and outputs the best values that allow the standardisation model to match the target (and therefore lower dispersion) as best as possible. The log likelihood was defined using the Equation:

$$-2\ln\mathcal{L} = \chi^2 + 2\sum_{i=1}^{N}\ln\sigma_i + N\ln(2\pi) \tag{16}$$

Where $\ln\mathcal{L}$ is the log likelihood, χ^2 the chi-squared statistic between the standardisation model and the target values, N is the number of objects in the dataset, and σ_i is the total error for each object. The sum term in Eq. 16 is a penalty term that stops the fitted values from blowing up. The prior ranges of α, β, γ and σ_{int} that the sampler explored were defined using the values obtained from the independent fits. The MCMC then used the log likelihoods and priors to explore the full posterior distribution for each parameter. Trace plots from the MCMC simultaneous fit were checked to ensure that all parameters had been adequately sampled and the walkers were well mixed.

The values of α, β and γ obtained by the simultaneous fit of the VLS are presented in Table 2. These are compared to the values obtained from the independent fits of the VLS and expected values in the literature. The intrinsic dispersions stated in Table 2 are for the VLS only. Table 2 demonstrates that standardisation parameters from the simultaneous fits are in better agreement with the expected values from the literature than the values derived from independent fits. This infers that the simultaneous fitting method is superior. The simultaneous fit also fits for σ_{int}. However, it is not possible to compare this to the simultaneously fitted value obtained by Ginolin et al. (2025a,b) for the VLS, because it has not yet been released at the time of writing. Alternatively, σ_{int} for a particular standardisation method can be estimated 'by hand' by applying the α, β and γ values from that method and using the algorithm discussed in Section 3.4.1. It may not be appropriate to compare a simultaneously fitted value of σ_{int} to an

estimate that was calculated by hand. Therefore, σ_{int} was also calculated by hand, using the values of α, β and γ from the simultaneous fit for direct comparison. This shows that σ_{int} for the VLS, calculated by hand, for the simultaneous fitting method, is in excellent agreement with the value calculated by hand using expected values. σ_{int} for the VLS is also not statistically significantly higher when using the independent fit parameters. This shows that even though independent fits do not produce optimal values of α, β and γ, these values do still successfully standardise the sample to a reasonable level. There is not enough statistical evidence from this investigation alone to confidently say that the independent fits are significantly worse at standardising the VLS sample. This is mainly due to the size of uncertainties in σ_{int} which would be improved by using a larger sample size. Another important result to comment on is that the value of σ_{int} obtained by the simultaneous fit is slightly different to the value to the value calculated by hand when using α, β and γ values from the simultaneous fits. This could suggest that the algorithm used to calculate σ_{int} by hand is not very accurate. Therefore, it would be best to only compare σ_{int} values that come directly from the simultaneous fit itself. As mentioned earlier this is unfortunately not possible when comparing independent fits. However, this rule was applied later when fitting for new corrections in Section 6.

Parameter	Independent Fit Value	Simultaneous Fit Value	Expected Value From Literature	Simultaneous Fit Values In Agreement With Literature?
α	0.119$\pm$0.007	0.150$\pm$0.008	0.161$\pm$0.01	0.867σ difference. Good agreement
β	2.94$\pm$0.04	3.01$\pm$0.05	3.05$\pm$0.06	0.51σ difference. Good agreement
γ	0.108$\pm$0.010	0.123$\pm$0.013	0.143$\pm$0.025	0.71σ difference. Good agreement
σ_{int} Calculated "By Hand"	0.196$\pm$0.006	0.194$\pm$0.006	0.193$\pm$0.006	0.12σ difference. Excellent Agreement
σ_{int} from Simultaneous Fit	N/A	0.199$\pm$0.006	N/A	N/A

Table 2: Standardisation parameters obtained from the simultaneous fits of the VLS compared to the independent fits of the VLS and expected values from the literature. The values of α, β and γ obtained by the simultaneous fits are in better agreement with the expected values than the ones obtained from independent fits. This is evidence that the simultaneous fitting method is better. However, when comparing σ_{int} of the VLS, calculated by hand, for each method, there is not enough statistical evidence to suggest that the independent fitting method is significantly worse. A larger sample size would be required to lower uncertainties in σ_{int} to obtain more statistical evidence.

Fig. 10 then shows a comparison between the DR2Cut sample standardised using independent fits versus simultaneous fits of the VLS. The σ_{int} value that being compared is calculated by hand. Fig. 10 shows that the standardisation parameters derived using simultaneous fits of the VLS produce a standardised sample of DR2cut with a σ_{int} that is 0.006 lower than that found for the DR2cut sample standardised using independent fits from the VLS. This shows that simultaneous fits are more effective at finding optimal values of α, β and γ than independent fits. However, due to the large uncertainties on σ_{int}, this reduction is only at the 1.1σ significance level. The uncertainty on σ_{int} can be reduced by using a larger sample size, which could lead to a more statistically significant result. A value of σ_{int} =0.162$\pm$0.004 for the DR2cut sample is also excellent agreement with the value obtained in Fig. 3, which used best α, β, γ values from the literature. This shows the simultaneous fitting method used in this investigation performs just as well as current state-of-the-art investigations. It is also interesting that the best value of σ_{int} for DR2cut (0.162$\pm$0.004) is significantly lower than the best value for

σ_{int} of the VLS (0.192±0.006) in Table 2. This 4.2σ significant difference might be because DR2cut contains double the number of objects than the VLS. This means any outliers in the low z region of the data have a bigger impact on the dispersion. This could be what is causing the intrinsic dispersion of the VLS to appear higher on average.

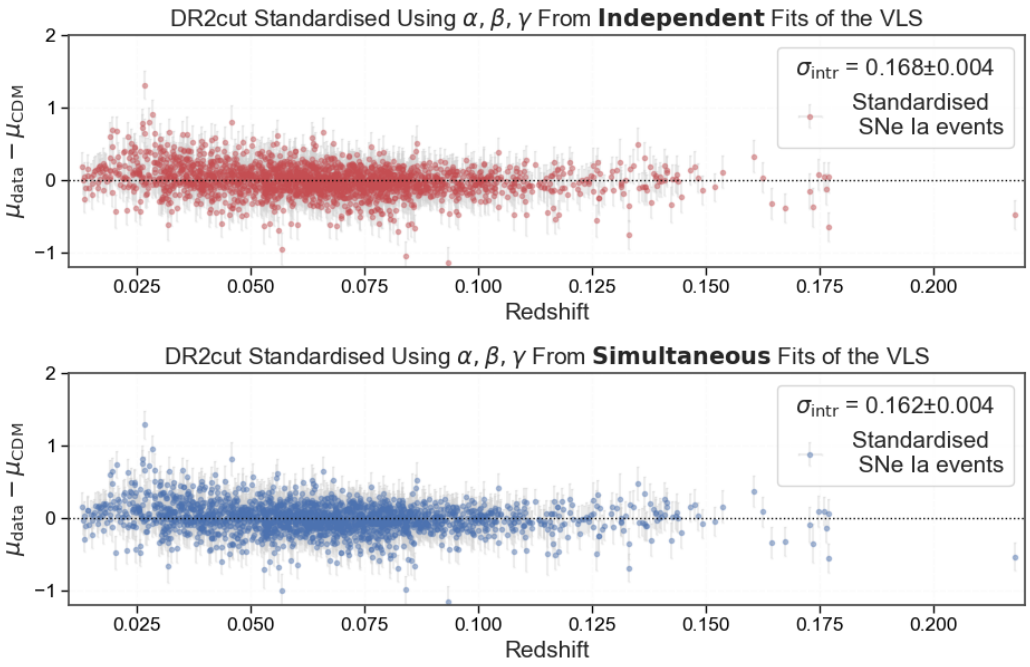

Figure 10: Hubble residuals of the DR2cut sample standardised using independent fits of the VLS (TOP) versus simultaneous fits of the VLS (BOTTOM). The intrinsic dispersion in DR2cut is reduced by a 1.1σ significant amount when using simultaneous fits instead of independent fits. This is because simultaneous fits find more optimal values of standardisation parameters. However, this reduction is not statistically significant. A larger sample size is needed to lower uncertainties in σ_{int} to confidently prove that simultaneous fitting is better.

To summarise, independent fits are a quick and simple way to derive values of α, β and γ that are quite close to the expected values. However, simultaneous fitting does perform slightly better because the standardisation parameters obtained from simultaneous fits are closer to the expected values. While there is not enough statistical evidence from this investigation to show that simultaneous fitting is significantly better at reducing σ_{int} than independent fitting for a given SNe Ia sample, simultaneous fitting was the method used for the rest of the investigation. This is because it is the method favoured by the literature and the values of σ_{int} obtained are more reliable.

5. Investigating Bias in the Full and SDA SNe Ia Samples

The VLS sample provided by Rigault et al. (2025) is free from selection bias (Amenouche et al., 2025). This means that the distributions of measured SNe Ia parameters from the VLS should represent their 'true' distribution. Therefore, the standardisation parameters derived from this sample can be found accurately without needing to include bias corrections. This is why the VLS was used throughout Section 4 to test the simultaneous and independent fitting routines. If the full DR2cut sample were to be used to derive standardisation parameters, a bias correction would be needed. This is because the full DR2cut sample is influenced by a selection

bias known as Malmquist bias. This is the preferential detection of intrinsically bright objects in astronomy. This is a problem for a sample of SNe Ia because their absolute brightnesses are not standard. Some SNe Ia appear fainter than others due to slight differences in their composition or environment and because of dust between the telescope and the event absorbing some light. If a certain minimum amount of light is required for an object to be detected, this could lead to some objects not being selected. Thus, a bias towards brighter objects is introduced, which may mean that the measured distributions of a sample do not reflect the true distributions. The objective of this section is to determine whether the SDA sample, which was used to find evidence for new corrections (see Section 6), is free from selection bias too. This is because a bias in the SDA sample might invalidate the results in Section 6 because the values of any new standardisation parameters discovered may not be accurate. If a bias correction is needed, then future work must be carried out to ensure that it does not significantly impact the results of this investigation.

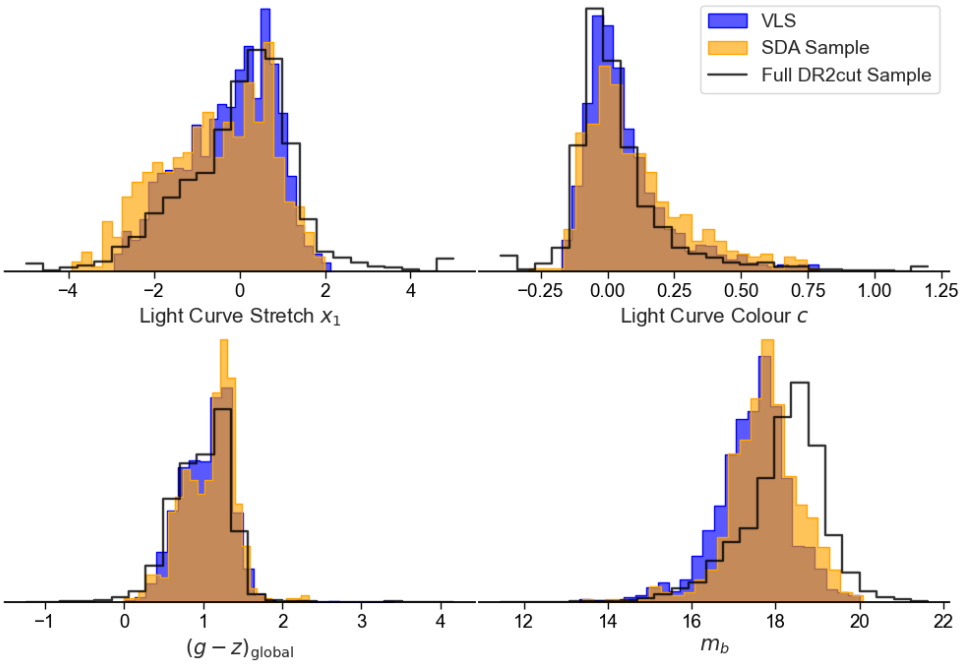

Figure 11: Distributions of the measured parameters of the SNe Ia used in this investigation for the 3 main samples used. The VLS is the non-biased sample and therefore should represent truth distributions. The distributions for the SDA sample and DR2cut appear to be different to the VLS distributions. There is a significant difference between m_b for DR2cut and the VLS. The distributions of x_1 all appear to be slightly different for each sample. A K-S test was performed on these distributions to determine whether the differences are statistically significant and the results are presented in Table 3.

The SDA sample is a subset of the VLS because it contains all the objects for which spectroscopic data is available at the $z \leq 0.06$ level. Therefore, it could be argued that it if the VLS is free from bias then so must the SDA sample. This is only true if the SDA sample is representative of the VLS. A representative sample means that the objects have been picked from random and the underlying distributions remain the same. However, the objects in the SDA sample may not have been picked at random. As discussed in Section 2.1, spectroscopy requires a lot of light to produce spectra. This means a telescope must observe the supernova for a long time to gather all the light it needs. If an object is not bright enough for a long enough time and a spectra cannot be produced, it is not selected in the sample and therefore a bias is introduced. However, there are other uncontrollable factors which may be lead to a spectrum

not being produced such as the weather. If it is too cloudy for a ground-based telescope (like the ones used by the ZTF) to operate efficiently, then not enough light can be detected to produce a spectrum. This means certain supernovae are not selected through random chance. It is therefore possible that the distributions of SNe Ia parameters are different for the SDA than the VLS because of random variation in the data. A statistical test was executed to determine if the distributions are significantly different or if the differences can be adequately explained by random data fluctuations.

Fig. 11 displays the distributions of measured SNe Ia parameters used in the standardisation process for the three different samples used in this investigation. A K-S test was performed to determine if the parameter distributions for the SDA sample are significantly different to the VLS distributions. The results from this test are presented in Table 3. The P-value determines whether the null hypothesis can be rejected. For this investigation the null hypothesis ($H0$) is: The parameter samples are drawn from the same distribution. If $P < 0.05$ then the null hypothesis is rejected, meaning the distributions are statistically significantly different.

Parameter	K-S Test P-value SDA vs VLS	Reject $H0$?	K-S Test P-value DR2cut vs VLS	Reject $H0$?
x_1	8e-5	Reject $H0$	2e-6	Reject $H0$
c	0.0006	Reject $H0$	5e-8	Reject $H0$
$(g-z)_{\text{global}}$	0.03	Reject $H0$	0.02	Reject $H0$
m_b	3e-5	Reject $H0$	4e-118	Reject $H0$

Table 3: The VLS is shown to be bias free and therefore has distributions of x_1,c,$(g-z)_{\text{global}}$ and m_b that are representative of the 'true' distributions. A K-S test was performed to compare the parameter distributions of DR2cut and the SDA sample to the VLS. The results from this test show that the distributions of the parameters in the DR2cut and SDA are significantly different to the VLS. This means that, as expected, DR2cut is biased. The SDA sample may also be biased which may impact the validity of the results in Section 6.

The results from the K-S tests in Table 3 shows that the DR2cut distributions are statistically significantly different to the VLS. This is expected because DR2cut is known to include a bias and therefore provides a good sanity check for the test. The SDA sample distributions are also shown to be significantly different to the VLS. This means that it is statistically very unlikely that the differences in the parameter distributions are caused by statistical fluctuations. Therefore, this suggests that there a may be a section bias present in the SDA sample. This is important to know because it may mean that the results obtained in Section 6, which uses the SDA sample, are not accurate. Determining the root cause of this selection bias and the form of a correction term needed to take this into account is beyond the scope of this project. Therefore, it is recommended that future studies investigate this further to determine if the results from Section 6 are valid.

6. Investigating the SDA Sample for new Spectroscopic Standardisation Corrections

This section investigates SNe Ia standardisation using spectroscopic data provided by Burgaz et al. (2025). There are 416 objects with spectroscopic data available, after applying the basic quality cuts discussed in Section 3.2, which make up the SDA sample used for this section. It is important to note that the results from Section 5 suggest that the SDA sample might be influenced by a selection bias. Therefore, any results from this section may need to be validated by

future studies that investigate and correct for this bias if it is found to have a significant impact on the results.

The spectroscopic data used in this section comes from the Silicon feature at 6355 Å in the spectra of SNe Ia. For each object in the SDA sample, there are values for Si II λ6355 velocities, pseudo-Equivalent Widths (pEW) and all associated uncertainties. There are no covariance terms provided which means error calculations will be estimated using only the error in the measured parameters. Silicon velocities correspond to the line-of-sight expansion velocities of the supernova ejecta. These are typically measured from the Doppler shift of the Si II λ6355 feature and are indicative of the explosion energy and conditions at the photosphere. PEWs are a way of quantifying the strength of an absorption feature by measuring its area. This provides insight into the composition of the star because a larger absorption feature could suggest that the element causing it is more abundant (however, absorption feature strength also depends on physical conditions such as temperature and ionisation). Both of these parameters provide more information on the nature of SNe Ia than photometrically measured parameters. If any correlations can be found, this could mean they could be used to correct for a deeper root cause of dispersion. This might improve the standardisation process which is very important for constraining cosmological parameters.

Corrections derived from spectroscopy would be a profound advancement for SNe Ia standardisation because their physical meaning is easier to interpret than controversial photometric corrections such as the host-step. It is possible that photometric or spectroscopic standardisation is correcting for the same root cause of dispersion but spectroscopic corrections are better in theory as they use more direct measurements of the supernovae. Another theoretical advantage for spectroscopic corrections is that, as discussed in Section 2.1, dust has less of an impact on the ability to interpret useful information from spectra than light-curves. Therefore, it is important to determine if it is possible to spot any correlations in the spectroscopic data. Independent fits of silicon velocity and pEW against standardised residuals were produced and the results illustrated in Sections 6.1 and 6.2. If a significant relationship was identified, simultaneous fitting was used to test if intrinsic dispersion can be lowered by using new models that incorporate these new corrections.

6.1 Silicon Velocity Correction

In order to test for a correlation using silicon velocity, the SDA sample must first be standardised using the classic photometric corrections. This means that any relationship that has not already been accounted for by these corrections will be visible on the independent fit. A simultaneous fit of the SDA sample, using the same method developed for the VLS in Section 4.5, was used to determine the photometric standardisation parameters α, β and γ. The values obtained for the simultaneous fit of the SDA were α = 0.157$\pm$0.012, β = 3.016$\pm$0.063 and γ = 0.158$\pm$0.02. These values are all in good agreement ($< 1\sigma$ difference) with the literature. Standardised Hubble residuals of the SDA were produced by applying these values to Eq. 10.

Fig. 12 shows the results of plotting standardised residuals against Si II λ6355 velocity for the SDA sample. The binned averages on Fig. 12 clearly show that there is no significant relationship observed between these parameters. The fitted linear function, with a gradient of zero to 4 significant figures, reinforces this. The error on the slope is of the same order of magnitude (10^{-6}) as the slope value itself, further proving that there is no significant linear relationship. No other functional forms appear to match the data. This concluded the investigation into silicon velocity because it was clear that no spectroscopic correction could be derived from this relationship. Therefore, pEW relationships were tested next.

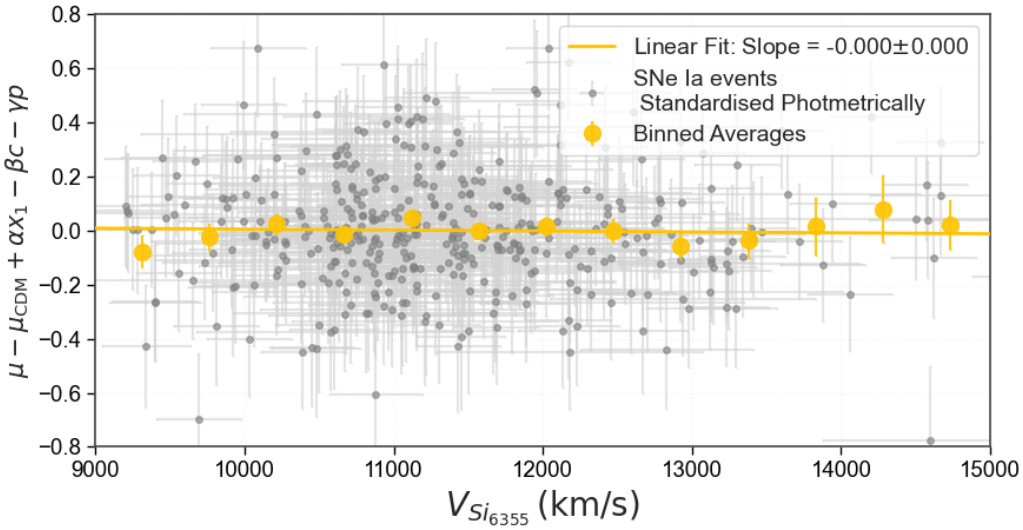

Figure 12: Independent fit of standardised Hubble residuals (corrected for light curve colour, stretch and global host colour) against silicon velocity for all objects from the SDA sample. A linear function was fitted to the data using 'scipy.optimize.curve_fit' in a Python program to determine if there was any significant relationship. Binned averages have been added to help visualise the data more clearly. There is no significant relationship observed between the two parameters. Therefore, silicon velocity cannot be used to create new spectroscopic standardisation parameters for the SDA sample.

6.2 Silicon Pseudo Equivalent Width (pEW) Correction

The same standardised Hubble residuals used in Section 6.1 were used to produce a plot of residuals against pEW for the SDA sample. The result is presented in Fig. 13. The binned averages on the plot suggested that there was a positive linear relationship between residuals and pEW. A linear function was fitted to the data to test if the slope was significant. The slope of the line of best fit was found to be 0.00163$\pm$0.00034 which is statistically significant at the 4.79σ level. This means that even after standardising for light curve stretch, colour and global host colour, a significant relationship can be still be identified on the independent fit of residuals against pEW. This provides evidence for a potential new standardisation correction parameter that takes this relationship into account. This new spectroscopic standardisation parameter will be called δ for this investigation and it is taken as the slope of the linear relationship observed between standardised residuals and pEW.

To test if δ was linked to any other parameters, Fig. 13 was recreated but with a different photometric standardisation parameter removed each time. When α was set to zero, the value of δ in Fig. 13 doubled in size to δ=0.00316$\pm$0.00034. When β was set to zero δ became 0.00092$\pm$0.0003 which is a reduction but still a significant slope at the 3.1σ level. Finally, when γ was set to zero the slope did not change significantly (δ=0.00153$\pm$0.00034). These tests imply that there are underlying relationships between the variables. Therefore, simultaneous fits using models that include δ were tested.

The first standardisation model involving δ that was tested in this investigation was a model that used δ as an alternative to the controversial γ correction. This is because the value of δ in the independent fit in Fig. 13 does not significantly change when γ is removed. This new

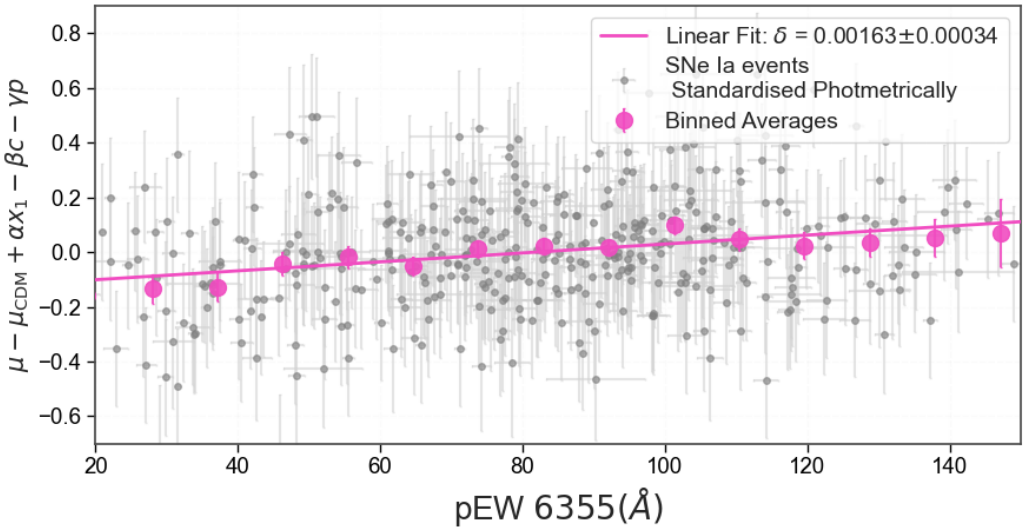

Figure 13: Independent fit of standardised Hubble residuals (corrected for light curve colour, stretch and global host colour) against silicon pEW for all objects from the SDA sample. A linear function was fitted to the data using 'scipy.optimize.curve_fit' to determine if there was any significant relationship. Binned averages have been added to help visualise the data more clearly. A significant linear relationship can be seen with a slope being found at the 4.66σ level. This could be evidence for a new spectroscopic standardisation correction.

model can be described by the expression:

$$\Delta\mu = \mu_{data} - \mu_{cosmo} = m_b - M - \mu_{cosmo} + \alpha x_1 - \beta c - \delta W_\lambda^* \tag{17}$$

where δ is the empirical spectroscopic standardisation parameter that corrects for the observed relationship between Hubble residuals and pseudo-equivalent width, which is denoted as W_λ^*. This notation is used to distinguish pEW from the commonly used symbol for normal equivalent widths (W_λ). The other model tested in this investigation was a model that includes δ as a fourth correction term on top of the α, β and γ terms. This is because Fig. 13 shows that there is still a relationship leftover that is not being accounted for by α, β and γ, therefore a fourth correction could reduce intrinsic dispersion. This model is described by the equation:

$$\Delta\mu = \mu_{data} - \mu_{cosmo} = m_b - M - \mu_{cosmo} + \alpha x_1 - \beta c + p\gamma - \delta W_\lambda^* \tag{18}$$

where α, β, γ and δ are empirical standardisation parameters that correct for the observed relationships between residuals and stretch x_1, colour c, host colour and pseudo-equivalent width W_λ^*. Also, p follows the same definition as stated in Eq. 9.

Now that the new δ models had been defined, in order to simultaneously fit for standardisation parameters and σ_{int} to test the effectiveness of each model, the error calculation from Eq. 15 also needed to be modified. The term $\delta\sigma_{W_\lambda^*}$ was added on in quadrature to Eq. 15 for any model that involves δ to include the error on pEW measurements. However, this investigation did not have access to covariances between pEW and SALT2 parameters like x_1,c and m_b. This means that the error is a best estimate only. This may lead to the σ_{int} values calculated for δ models being overestimated because the base error is technically too small when it does not include covariance terms. It is recommended that future investigations devote more time to include the covariance terms in the error definition to see if they have a significant impact on the σ_{int} value obtained.

Simultaneous fits of the SDA sample using the MCMC method outlined in Section 4.5 were executed for the new models described in Eqs. 17 and 18. The standardisation parameters and values of σ_{int} they obtained were compared to the values obtained using simultaneous fits of the widely-accepted photometric standardisation models. Standard deviations of each standardised sample were also calculated. The results are presented in Table 4. The α,β,δ model from Eq. 17 is shown to standardise the SDA sample just as effectively as the α,β,γ model from Eq. 15, however it does not improve upon it. This is because the values of σ_{int} they both obtain are statistically similar (0.31σ difference). The α,β,γ,δ model from Eq. 18 does improve upon the σ_{int} value obtained by the α,β,γ model with a 0.011 reduction. However, due to the large uncertainties in σ_{int} this reduction is only 0.86σ significant. Nevertheless, a δ correction parameter of δ=0.0018$\pm$0.00036 which is 5σ significant is still found by the simultaneous fit for this model. There is not enough statistical evidence from this investigation to determine if this significant δ correction can effectively lower σ_{int} in the SDA sample by a statistically significant amount. The standard deviation of the sample is lowest when using the α,β,γ,δ model, which could provide evidence that this is the better model. Section 7 discusses the possible physical origin of the δ correction, how it is linked to other corrections and what measures could be taken by future investigations to find more conclusive evidence that δ can improve standardisation. Cosmological implications are also discussed.

Model Used	α	β	γ	δ	σ_{int}	STD
No standardisation	–	–	–	–	0.578$\pm$0.02	0.579
α,β (Eq. 7)	0.104$\pm$0.010	2.96$\pm$0.06	–	–	0.201$\pm$0.009	0.236
α,β,γ(Eq. 10)	0.157$\pm$0.012	3.02$\pm$0.06	0.158$\pm$0.020	–	0.187$\pm$0.009	0.228
α,β,δ(Eq. 17)	0.105$\pm$0.010	2.96$\pm$0.06	–	0.00203$\pm$0.00036	0.191$\pm$0.009	0.227
α,β,γ,δ(Eq. 18)	0.142$\pm$0.012	3.03$\pm$0.06	0.147$\pm$0.020	0.0018$\pm$0.00036	**0.176$\pm$0.009**	**0.221**

Table 4: Results from MCMC simultaneous fits for different standardisation models applied to the SDA sample. A significant δ value is identified in both models that employ the new correction. However, there is not enough statistical evidence from this investigation yet to say whether δ corrections can improve standardisation by lowering σ_{int} by significant amount.

7. Discussion

7.1 Physical Origins of the pEW Correction

Section 6.2 demonstrated that a significant linear relationship between photometrically standardised residuals and Si II λ6355 pEW exists. A MCMC simultaneous fit for all standardisation parameters obtains a value of the new linear pEW correction (δ) that is significant at the 5σ level. It is unclear whether this new correction significantly lowers the intrinsic dispersion and therefore improves the standardisation of the sample. This is discussed further in Section 7.2. This section looks deeper in to the possible physical meaning behind a pEW correction and investigates how it may be related to other corrections.

The independent fit of residuals against pEW in Fig. 13 shows that the linear relationship has a positive correlation. However, since magnitudes (brightnesses) are defined in astronomy as brighter objects having a more negative value, this suggests that SNe Ia with a higher Si II λ6355 pEW value in the SDA sample, are on average less bright (after photometric standardisation). This comes from the fact that plotting residuals on the y-axis is essentially the same thing as plotting absolute magnitudes. Residuals are just centred around zero for easier

analysis. This raises an important question: Why is a higher value Si II λ6355 pEW linked to lower brightness?

This relationship could be explained by a result from Burgaz et al. (2025) which states that "SNe Ia with lower pEW ratios tend to have faster declining light curves". PEW ratio is defined as:

$$\text{pEW ratio} = \frac{\text{pEW Si}_{II}\,\lambda 5972}{\text{pEW Si}_{II}\,\lambda 6355} \tag{19}$$

where another prominent Silicon feature at 5972 Å in the spectra of SNe Ia is used to define the ratio along with the main feature at 6355 Å used in this investigation. If a lower pEW ratio is linked to a faster declining light curve, this means that SNe Ia with a higher pEW ratio have wider light curves. A wider light curve means a brighter object. This means the result found in Section 6.2 is consistent with the findings from Burgaz et al. (2025). This is because Fig. 13 shows that SNe Ia with a higher Si II λ6355 pEW value in the SDA sample, are on average less bright. A lower value of Si II λ6355 pEW means a higher pEW ratio because this is the denominator of the fraction. Burgaz et al. (2025) shows that a higher pEW ratio is paired with a brighter object, this investigation shows that a lower Si II λ6355 pEW, which causes a higher pEW ratio, is also paired with a brighter object. Therefore, the results are consistent. However, it is important to remember that pEW ratio also depends on Si II λ5972 pEW.

If the δ correction is linked to pEW ratio then this could reveal more about the origin of this correction. PEW ratio of the Si II features is known to be a good empirical temperature indicator (e.g., Hachinger et al., 2008). Burgaz et al. (2025) suggest that there is a strong relation between the mass of radioactive nickel (^{56}Ni) and temperature of the ejecta, where SNe Ia with more ^{56}Ni have hotter ejecta. The absolute magnitude of a SNe Ia event is directly driven by the amount of ^{56}Ni produced in the explosion. As discussed in Section 2.1 it is the high energy photons from the radioactive decay of elements like nickel that cause the peak brightness observed in SNe Ia events. This means that the δ correction might be linked more directly to deeper route causes of SNe Ia brightness dispersion than photometric corrections. This means that even though there is not enough evidence that this correction significantly improves SNe Ia standardisation yet, this investigation shows that it has a tremendous potential to do so. Therefore, it is recommended that further studies dedicate more time into investigating spectroscopic corrections. More detailed suggestions for future work are addressed in Section 7.4.

The δ correction may also be correlated with other correction parameters like x_1 that take light curve width, and therefore intrinsic brightness into account. A corner plot from the simultaneous fit of α, β, γ and δ was produced to identify any underlying relationships between parameters in the fit. Fig. 14 shows the results of this corner plot. δ appears to be linked to α due to the ellipsoidal shape of the distribution observed in the lower left panel. This is reinforced by the idea that the δ correction appeared to become stronger when α was removed in the independent fit, as discussed in Section 6.2. This relationship could suggest that α and δ correct for the same phenomena and a model which replaces α with δ would be good to test in future investigations. The γ correction remains controversial as this is seen to have a very strong correlation with α too in the left-middle panel of Fig. 14.

7.2 Can Spectroscopic Data Improve SNe Ia Standardisation?

This investigation showed that there is a significant relationship between photometrically standardised residuals and Si II λ6355 pEW for the SDA sample. However, there is not enough evidence to show that using this correction significantly improves upon current SNe Ia standardisation. The standard deviation in the SDA sample is lowered when using the new model

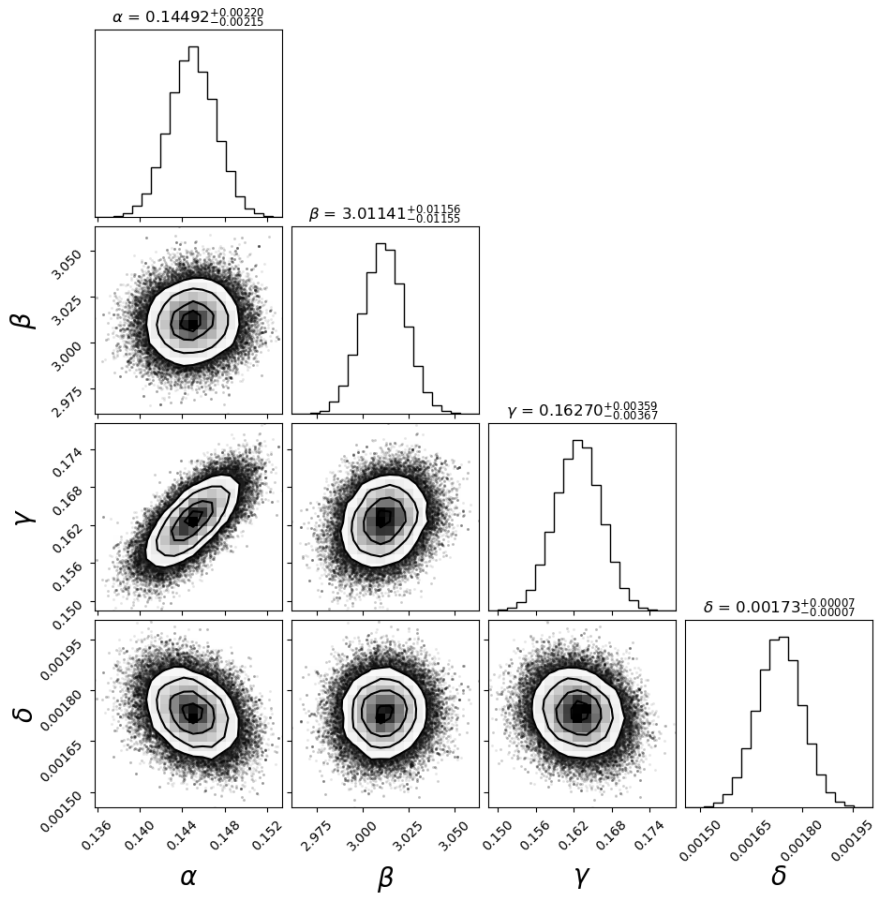

Figure 14: Corner plot distributions from the MCMC simultaneous fit of the standardisation parameters α, β, γ and δ for the SDA sample. A strong correlation between γ and α and a slight correlation between δ and α is observed .

that inlcudes δ, but σ_{int} is not lowered significantly. This shows is that spectroscopic data has great potential and should be investigated further. There are several problems with this investigation which may lead to the inconclusive results for σ_{int}. If these problems are addressed, it may provide stronger evidence that the spectroscopic corrections identified in this investigation are useful.

Firstly, Section 5 showed that there may be a selection bias present in the SDA sample used to derive the new spectroscopic correction. This means a bias correction may need to be included which might impact the final results. There were also no covariance terms between pEW and light curve measurements such as x_1 or c included in the error definition of models that use the δ correction. This means the estimate for intrinsic dispersion for these models might be overestimated. If intrinsic dispersion is found to actually be reduced more when these terms are included it may lead to the results being more statistically significant. Another issue that is causing the results to be inconclusive is the size of the uncertainties in the simultaneously fitted values of σ_{int}. The α,β,γ,δ model lowers the σ_{int} of the SDA sample by a value of 0.011 compared to the α,β,δ model. However, this is statistically insignificant when the errors of these values are of the order of $\sim$ 0.009. This uncertainty is caused by the smaller sample size of the SDA, which comprises of 416 objects. The uncertainties of σ_{int} values for the DR2cut sample are usually found with a precision of 0.003. This sample contains $\sim$ 2000 objects. If the SDA sample size was increased to this size and the uncertainties were lowered to a similar amount, it may become more clear if the α,β,γ,δ model is superior. Also, a value of σ_{int} =0.176$\pm$0.009

obtained by the α,β,γ,δ model for the SDA sample is higher than the expected value in the literature ($\sim$ 0.15). This might be because outliers in the SDA sample are causing the dispersion to increase, which has more of an impact on a smaller sample like the SDA. However, this does not change the result of this investigation because the intrinsic dispersions using any model to standardise SDA is increased by the same amount, meaning internal comparison is still possible. To produce σ_{int} values that are comparable to the literature, outliers may have to be removed via a process such as Chauvenet's criterion.

SNe Ia spectra need more light to be produced than a photometric light curve, which takes up more valuable time on telescopes. This means spectroscopy is more expensive than photometry. It is important to know if it is worth the extra expense to gather more spectroscopic data. This investigation shows that spectroscopic data has the potential to reveal better SNe Ia standardisation corrections. Therefore, spectral analysis is worth investing in. However, other studies must be carried out to validate and expand upon the results from this investigation. If standardisation can be improved, this has good implications for cosmology, which is discussed in the next section.

7.3 Cosmological Implications

If spectroscopic corrections can be shown to improve the standardisation of a SNe Ia sample, this means measurements of cosmological parameters can be constrained even further. This is because SNe Ia are used as 'standardisable' candles to calibrate distance measurements. After a sample has been standardised, the average absolute brightness of SNe Ia in the sample is used to calibrate the distance to other objects. This means if standardisation is improved and the brightness dispersion is lowered, a more reliable average absolute brightness can be calculated. This means distance measurements are more accurate. Accurate distance measurements are so important because they are used to calculate cosmological parameters like the Hubble-Lemaître constant H_0, the mass density parameter Ω_m and the dark energy equation of state parameter ω. One of the ways this can be done is by producing a Hubble diagram of the data and comparing it to a cosmology model. If the data matches the cosmology model well, then this infers that the cosmological parameters that model uses are a good fit. Fig. 15 demonstrates how standardised distance moduli allow a parameter such as H_0 to be constrained. This is a basic example used to emphasise the fact that if the standardisation of the sample is improved, the constraints on parameters like H_0 can be narrowed, which improves cosmology.

7.4 Future Work

This investigation found evidence for a significant relationship between standardised Hubble residuals and Si II λ6355 pEW. A new spectroscopic standardisation correction was derived from this relationship and a new standardisation model was tested on the SDA sample. It is not yet clear if the new models improve upon current standardisation techniques and some of the results from this investigation may need to be validated. However, spectroscopic data has a great potential to improve SNe Ia standardisation.

If future studies are to be dedicated to spectroscopic standardisation this report recommends that the largest sample size possible is used to limit uncertainties. Future studies must also check that their sample is not biased like the SDA. If a significant bias is found, then corrections may need to be included so that results are accurate. Also, covariance terms between spectroscopic and photometric measurements must be included in the error calculation to ensure σ_{int} is accurate. A further detailed analysis on the relationship the δ correction has with

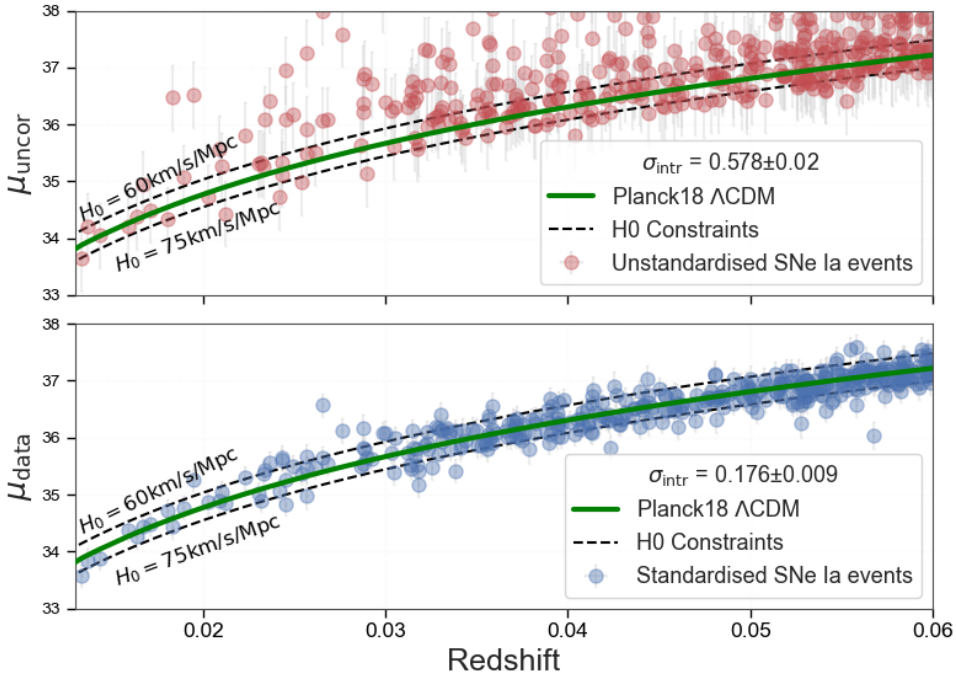

Figure 15: Hubble diagrams of the unstandardised SDA sample (TOP) compared to the standardised SDA sample using simultaneously fitted standardisation parameters from the α,β,γ,δ model. The λCDM cosmology model with different values of H_0 has been included to demonstrate how Hubble diagrams can be used to constrain cosmological parameters.

other parameters could be performed, as this investigation shows that there may be underlying correlations. Other models involving δ such as model that uses δ as a replacement for α could be tested. This report did not exhaustively test all spectroscopic data available for SNe Ia. It is possible that other more potent spectroscopic corrections could be found between other spectroscopic features such as pEW ratios, or Si II λ5972 pEW. Spectroscopy uses more direct measurements from the SNe Ia than photometry which means it has the potential to correct for deeper root causes of SNe Ia brightness dispersion. More studies must be dedicated to build upon the work in this report to conclusively determine if spectroscopic standardisation can improve photometric standardisation.

8. Conclusions

This report presents a detailed analysis of possible ways in which the standardisation of SNe Ia can be improved. The objective of this investigation was to determine whether spectroscopic data can be used to improve photometric standardisation. Using SNe Ia data from the ZTF DR2 sample provided by Rigault et al. (2025), current photometric standardisation methods were evaluated. Then, spectroscopic data for a subset of the ZTF DR2 sample provided by Burgaz et al. (2025) was examined to search for potential spectroscopic standardisation corrections that could refine SNe Ia standardisation. Finding ways to enhance the standardisation process is crucial because it improves the accuracy of cosmic distance measurements. This means cosmological parameters can be constrained further and our understanding of the universe as a whole is improved. The conclusions from this investigation are the following:

1) Host colour is a more reliable environmental tracer than host mass for deriving the γ correc-

tion suggested by Sullivan et al. (2010) because the expected functional form (a step function) is clearer in the independent plot of residuals against host colour.
2) Simultaneous fitting is the optimal method to derive the values of standardisation parameters because it takes underlying relationships into account. However, independent fits to provide a good estimate and are easier to produce.
3) The sample of SNe Ia with spectroscopic data available (SDA sample) may be influenced by a non-random selection bias. This is because the distributions of photometrically measured SNe Ia parameters such as stretch x_1, colour c, host colour $(g-z)$ and apparent magnitude m_b are statistically significantly different to the expected distributions of these parameters in the Volume Limited Sample (VLS) provided by Rigault et al. (2025). The VLS is known to be bias free and is therefore representative of "truth" distributions (Amenouche et al., 2025). Future studies should investigate whether this bias has a significant impact on the results and if a bias correction may be required.
4) There was no significant relationship observed in the independent fit of photometrically standardised SNe Ia Hubble residuals against Si II λ6355 velocity. Therefore, a standardisation correction could not be derived using this data.
5) A significant linear relationship was observed in the independent fit of photometrically standardised SNe Ia Hubble residuals against Si II λ6355 pEW. A linear function was fitted to the data and a slope of 0.00163$\pm$0.00034, which is 4.79σ significant, was found.
6) A new spectroscopic standardisation correction δ is proposed that could correct for the observed relationship between residuals and pEW. A refined standardisation model that includes this as a fourth correction alongside the widely used photometric corrections ($\alpha\beta\gamma$) was tested. A simultaneous MCMC fit for α, β, γ, δ and σ_{int} yielded a δ value of 0.0018$\pm$0.00036 which is significant at the 5σ level.
7) The $\alpha\beta\gamma\delta$ model standardised the SDA sample such that the standard deviation was 0.221 and σ_{int}=0.176$\pm$0.009. These are both an improvement upon the values obtained by the current widely used photometric standardisation model which uses only $\alpha\beta\gamma$ (STD=0.228, σ_{int}=0.187$\pm$0.009). However, due to the large uncertainties in the σ_{int} values obtained by the simultaneous fits for each model, the reduction in σ_{int} is only 0.86σ significant. This means there is not enough statistical evidence from this investigation to confirm if the $\alpha\beta\gamma\delta$ model significantly improves SNe Ia standardisation.

This report highlights the fact that spectroscopic data has a great potential to improve SNe Ia standardisation. If spectroscopic corrections, such as ones like δ suggested by this investigation, can be shown to significantly reduce the dispersion in an SNe Ia sample, this will enhance SNe Ia standardisation considerably. Spectroscopic data has unique advantages over photometric data such as the fact that it uses more direct measurements from the SNe Ia themselves. Therefore, spectroscopic corrections could correct for a deeper root cause of observed SNe Ia brightness dispersion than photometric corrections, and their physical origins are easier to understand. A significant correction parameter was discovered using spectroscopic data in this investigation. This report emphasises the need to explore this further to conclusively determine if SNe Ia standardisation can be improved. This work lays a foundation for future studies to expand and robustly test spectroscopic SNe Ia standardisation corrections so that the ultimate goal of improving distance measurements and advancing cosmological understanding is achieved.

Acknowledgements

Firstly, I express my sincere thanks to my supervisor, Dr. Mathew Smith, from the Department of Physics, Lancaster University, Lancs LA1 4YB, UK for their guidance and support throughout this research project.

This project made use of the second data release associated with the “Type Ia Supernovae & Cosmology” science working group, aka “DR2”, based on observations obtained with the Samuel Oschin Telescope 48-inch and the 60-inch Telescope at the Palomar Observatory as part of the Zwicky Transient Facility project.

Finally, I sincerely thank my family and friends for their continued support and encouragement throughout my studies at Lancaster University, without which this project may not have been possible.

References

Amenouche, M., Rosnet, P., Smith, M., Rigault, M., Aubert, M., Barjou-Delayre, C., Burgaz, U., Carreres, B., Dimitriadis, G., Feinstein, F., et al. (2025). Ztf sn ia dr2: Simulations and volume-limited sample. *Astronomy & Astrophysics*, 694:A3.

Astropy Collaboration, Robitaille, T. P., Tollerud, E. J., et al. (2013). Astropy: A community Python package for astronomy. , 558:A33.

Bailey, S., Aldering, G., Antilogus, P., Aragon, C., Baltay, C., Bongard, S., Buton, C., Childress, M., Chotard, N., Copin, Y., et al. (2009). Using spectral flux ratios to standardize sn ia luminosities. *Astronomy & Astrophysics*, 500(2):L17–L20.

Bellm, E. C., Kulkarni, S. R., Graham, M. J., Dekany, R., Smith, R. M., Riddle, R., Masci, F. J., Helou, G., Prince, T. A., Adams, S. M., et al. (2018). The zwicky transient facility: system overview, performance, and first results. *Publications of the Astronomical Society of the Pacific*, 131(995):018002.

Betoule, M., Kessler, R., Guy, J., Mosher, J., Hardin, D., Biswas, R., Astier, P., El-Hage, P., Konig, M., Kuhlmann, S., et al. (2014). Improved cosmological constraints from a joint analysis of the sdss-ii and snls supernova samples. *Astronomy & Astrophysics*, 568:A22.

Branch, D. and Tammann, G. (1992). Type ia supernovae as standard candles. *In: Annual review of astronomy and astrophysics. Vol. 30 (A93-25826 09-90), p. 359-389.*, 30:359–389.

Briday, M., Rigault, M., Graziani, R., Copin, Y., Aldering, G., Amenouche, M., Brinnel, V., Kim, A., Kim, Y.-L., Lezmy, J., et al. (2022). Accuracy of environmental tracers and consequences for determining the type ia supernova magnitude step. *Astronomy & Astrophysics*, 657:A22.

Brout, D. and Riess, A. (2024). The impact of dust on cepheid and type ia supernova distances. *The Hubble Constant Tension*, pages 363–383.

Brout, D., Scolnic, D., Popovic, B., Riess, A. G., Carr, A., Zuntz, J., Kessler, R., Davis, T. M., Hinton, S., Jones, D., et al. (2022). The pantheon+ analysis: cosmological constraints. *The Astrophysical Journal*, 938(2):110.

Burgaz, U., Maguire, K., Dimitriadis, G., Harvey, L., Senzel, R., Sollerman, J., Nordin, J., Galbany, L., Rigault, M., Smith, M., et al. (2025). Ztf sn ia dr2: The spectral diversity of type ia supernovae in a volume-limited sample. *Astronomy & Astrophysics*, 694:A9.

Carroll, B. W. and Ostlie, D. A. (2017). *An Introduction to Modern Astrophysics*. Cambridge University Press, second edition. edition.

Chandrasekhar, S. (1931). The maximum mass of ideal white dwarfs. *Astrophysical Journal, vol. 74, p. 81*, 74:81.

Chung, C., Park, S., Son, J., Cho, H., and Lee, Y.-W. (2024). Strong progenitor age bias in supernova cosmology. i. robust and ubiquitous evidence from a larger sample of host galaxies in a broader redshift range. *arXiv preprint arXiv:2411.05299*.

Collaboration, P. (2020). N. aghanim et al. *arXiv preprint arXiv:1807.06209*.

Dekany, R., Smith, R. M., Riddle, R., Feeney, M., Porter, M., Hale, D., Zolkower, J., Belicki, J., Kaye, S., Henning, J., et al. (2020). The zwicky transient facility: Observing system. *Publications of the Astronomical Society of the Pacific*, 132(1009):038001.

DESI Collaboration, D. (2025). Desi 2024 vi: Cosmological constraints from the measurements of baryon acoustic oscillations. *Journal of Cosmology and Astroparticle Physics*, 2025(02):021.

Dixon, M., Lidman, C., Mould, J., Kelsey, L., Brout, D., Möller, A., Wiseman, P., Sullivan, M., Galbany, L., Davis, T., et al. (2022). Using host galaxy spectroscopy to explore systematics in the standardization of type ia supernovae. *Monthly Notices of the Royal Astronomical Society*, 517(3):4291–4304.

Dixon, S. (2021). Biases from non-simultaneous regression with correlated covariates: A case study from supernova cosmology. *Publications of the Astronomical Society of the Pacific*, 133(1023):054501.

Freedman, W. L. (2021). Measurements of the hubble constant: tensions in perspective. *The Astrophysical Journal*, 919(1):16.

Gal-Yam, A. (2016). Observational and physical classification of supernovae. *arXiv preprint arXiv:1611.09353*.

Ginolin, M., Rigault, M., Copin, Y., Popovic, B., Dimitriadis, G., Goobar, A., Johansson, J., Maguire, K., Nordin, J., Smith, M., et al. (2025a). Ztf sn ia dr2: Colour standardisation of type ia supernovae and its dependence on the environment. *Astronomy & Astrophysics*, 694:A4.

Ginolin, M., Rigault, M., Smith, M., Copin, Y., Ruppin, F., Dimitriadis, G., Goobar, A., Johansson, J., Maguire, K., Nordin, J., et al. (2025b). Ztf sn ia dr2: Environmental dependencies of stretch and luminosity for a volume-limited sample of 1000 type ia supernovae. *Astronomy & Astrophysics*, 695:A140.

Guy, J., Astier, P., Baumont, S., Hardin, D., Pain, R., Regnault, N., Basa, S., Carlberg, R., Conley, A., Fabbro, S., et al. (2007). Salt2: using distant supernovae to improve the use of type ia supernovae as distance indicators. *Astronomy & Astrophysics*, 466(1):11–21.

Hachinger, S., Mazzali, P. A., Tanaka, M., Hillebrandt, W., and Benetti, S. (2008). Spectral luminosity indicators in type ia supernovae. understanding the (si ii) line-strength ratio and beyond. *Monthly Notices of the Royal Astronomical Society*, 389(3):1087–1096.

Hamuy, M., Phillips, M., Maza, J., Suntzeff, N. B., Schommer, R., and Aviles, R. (1995). A hubble diagram of distant type ia supernovae. *The Astronomical Journal (ISSN 0004-6256), vol. 109, no. 1669, p. 1-13*, 109:1–13.

Harkness, R. P. and Wheeler, J. C. (1990). Classification of supernovae. In *Supernovae*, pages 1–29. Springer.

Hillebrandt, W. and Niemeyer, J. C. (2000). Type ia supernova explosion models. *Annual Review of Astronomy and Astrophysics*, 38(1):191–230.

Iben Jr, I. and Tutukov, A. V. (1984). Supernovae of type i as end products of the evolution of binaries with components of moderate initial mass (m not greater than about 9 solar masses). *Astrophysical Journal Supplement Series (ISSN 0067-0049), vol. 54, Feb. 1984, p. 335-372.*, 54:335–372.

Jha, S. W., Maguire, K., and Sullivan, M. (2019). Observational properties of thermonuclear supernovae. *Nature Astronomy*, 3(8):706–716.

Kato, M., Saio, H., and Hachisu, I. (2018). Production of silicon on mass-increasing white dwarfs: Possible origin of high-velocity features in type ia supernovae. *The Astrophysical Journal*, 863(2):125.

Kelly, P. L., Hicken, M., Burke, D. L., Mandel, K. S., and Kirshner, R. P. (2010). Hubble residuals of nearby type ia supernovae are correlated with host galaxy masses. *The Astrophysical Journal*, 715(2):743.

Kessler, R. and Scolnic, D. (2017). Correcting type ia supernova distances for selection biases and contamination in photometrically identified samples. *The Astrophysical Journal*, 836(1):56.

Kim, Y.-L., Smith, M., Sullivan, M., and Lee, Y.-W. (2018). Environmental dependence of type ia supernova luminosities from a sample without a local–global difference in host star formation. *The Astrophysical Journal*, 854(1):24.

Liu, Z.-W., Röpke, F. K., and Han, Z. (2023). Type ia supernova explosions in binary systems: A review. *Research in Astronomy and Astrophysics*, 23(8):082001.

Maoz, D., Mannucci, F., and Nelemans, G. (2014). Observational clues to the progenitors of type ia supernovae. *Annual Review of Astronomy and Astrophysics*, 52(1):107–170.

Martin, B., Lidman, C., Brout, D., Tucker, B., Dixon, M., and Armstrong, P. (2024). [o ii] as an effective indicator of the dependence between the standardized luminosities of type ia supernovae and the properties of their host galaxies. *Monthly Notices of the Royal Astronomical Society*, 533(3):2640–2655.

Mazzali, P. A., Ropke, F. K., Benetti, S., and Hillebrandt, W. (2007). A common explosion mechanism for type ia supernovae. *Science*, 315(5813):825–828.

Nugent, P. E., Sullivan, M., Cenko, S. B., Thomas, R. C., Kasen, D., Howell, D. A., Bersier, D., Bloom, J. S., Kulkarni, S., Kandrashoff, M. T., et al. (2011). Supernova sn 2011fe from an exploding carbon–oxygen white dwarf star. *Nature*, 480(7377):344–347.

Perlmutter, S., Aldering, G., Goldhaber, G., Knop, R. A., Nugent, P., Castro, P. G., Deustua, S., Fabbro, S., Goobar, A., Groom, D. E., et al. (1999). Measurements of ω and λ from 42 high-redshift supernovae. *The Astrophysical Journal*, 517(2):565.

Phillips, M. M. (1993). The absolute magnitudes of type ia supernovae. *Astrophysical Journal, Part 2-Letters (ISSN 0004-637X), vol. 413, no. 2, p. L105-L108.*, 413:L105–L108.

Planck Collaboration, P. (2020). Planck 2018 results-vi. cosmological parameters. *Astronomy & Astrophysics*, 641:A6.

Price-Whelan, A. M. et al. (2018). The Astropy Project: Building an Open-science Project and Status of the v2.0 Core Package. , 156:123.

Riess, A. G., Filippenko, A. V., Challis, P., Clocchiatti, A., Diercks, A., Garnavich, P. M., Gilliland, R. L., Hogan, C. J., Jha, S., Kirshner, R. P., et al. (1998). Observational evidence from supernovae for an accelerating universe and a cosmological constant. *The astronomical journal*, 116(3):1009.

Riess, A. G., Press, W. H., and Kirshner, R. P. (1996). A precise distance indicator: Type ia supernova multicolor light-curve shapes. *The Astrophysical Journal*, 473(1):88.

Riess, A. G., Yuan, W., Macri, L. M., Scolnic, D., Brout, D., Casertano, S., Jones, D. O., Murakami, Y., Anand, G. S., Breuval, L., et al. (2022). A comprehensive measurement of the local value of the hubble constant with 1 km s- 1 mpc- 1 uncertainty from the hubble space telescope and the sh0es team. *The Astrophysical journal letters*, 934(1):L7.

Rigault, M., Smith, M., Goobar, A., Maguire, K., Dimitriadis, G., Johansson, J., Nordin, J., Burgaz, U., Dhawan, S., Sollerman, J., et al. (2025). Ztf sn ia dr2: Overview. *Astronomy & Astrophysics*, 694:A1.

Rose, B., Dixon, S., Rubin, D., Hounsell, R., Saunders, C., Deustua, S., Fruchter, A., Galbany, L., Perlmutter, S., and Sako, M. (2020). Initial evaluation of snemo2 and snemo7 standardization derived from current light curves of type ia supernovae. *The Astrophysical Journal*, 890(1):60.

Rose, B., Rubin, D., Strolger, L., and Garnavich, P. (2021). Host galaxy mass combined with local stellar age improve type ia supernovae distances. *The Astrophysical Journal*, 909(1):28.

Rose, B. M., Popovic, B., Scolnic, D., and Brout, D. (2022). Constraining rv variation using highly reddened type ia supernovae from the pantheon+ sample. *Monthly Notices of the Royal Astronomical Society*, 516(4):4822–4832.

Sullivan, M., Conley, A., Howell, D., Neill, J., Astier, P., Balland, C., Basa, S., Carlberg, R., Fouchez, D., Guy, J., et al. (2010). The dependence of type ia supernovae luminosities on their host galaxies. *Monthly Notices of the Royal Astronomical Society*, 406(2):782–802.

Taylor, G., Lidman, C., Tucker, B., Brout, D., Hinton, S., and Kessler, R. (2021). A revised salt2 surface for fitting type ia supernova light curves. *Monthly Notices of the Royal Astronomical Society*, 504(3):4111–4122.

Tripp, R. (1998). A two-parameter luminosity correction for type ia supernovae. *Astronomy and Astrophysics, v. 331, p. 815-820 (1998)*, 331:815–820.

Wheeler, J. C. and Harkness, R. P. (1990). Type i supernovae. *Reports on Progress in physics*, 53(12):1467.

Whelan, J. and Iben Jr, I. (1973). Binaries and supernovae of type i. *Astrophysical Journal, Vol. 186, pp. 1007-1014 (1973)*, 186:1007–1014.

Wiseman, P., Sullivan, M., Smith, M., and Popovic, B. (2023). Further evidence that galaxy age drives observed type ia supernova luminosity differences. *Monthly Notices of the Royal Astronomical Society*, 520(4):6214–6222.